University of Nottingham
UK | CHINA | MALAYSIA

GRAVITY LABORATORY

UKRI Science and Technology Facilities Council

@gravity_laboratory

Analogue Gravity 2026, Benasque, 14 January 2026

Exploring nonlinear wave interactions in classical and quantum fluid dynamical simulators

Silvia Schiattarella
silvia.schiattarella@nottingham.ac.uk

Collaboration:
S. Gregory, B. Macpherson, P. Smaniotto, V. B. Silveira, L. Solidoro, A. Avgoustidis, S. Weinfurtner

Analogue Simulators

Gondret, V. *et al*, *PRL*, **135**, 240603 (2025)

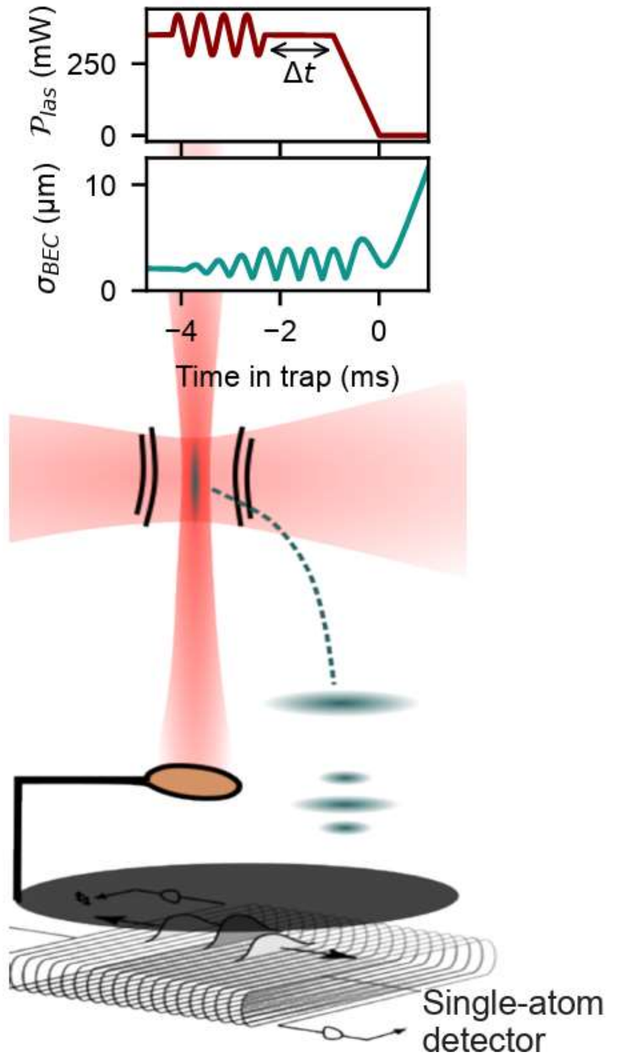

Steinhauer, J. ,*Nat. Phys.*, **12**, 959–965 (2016)

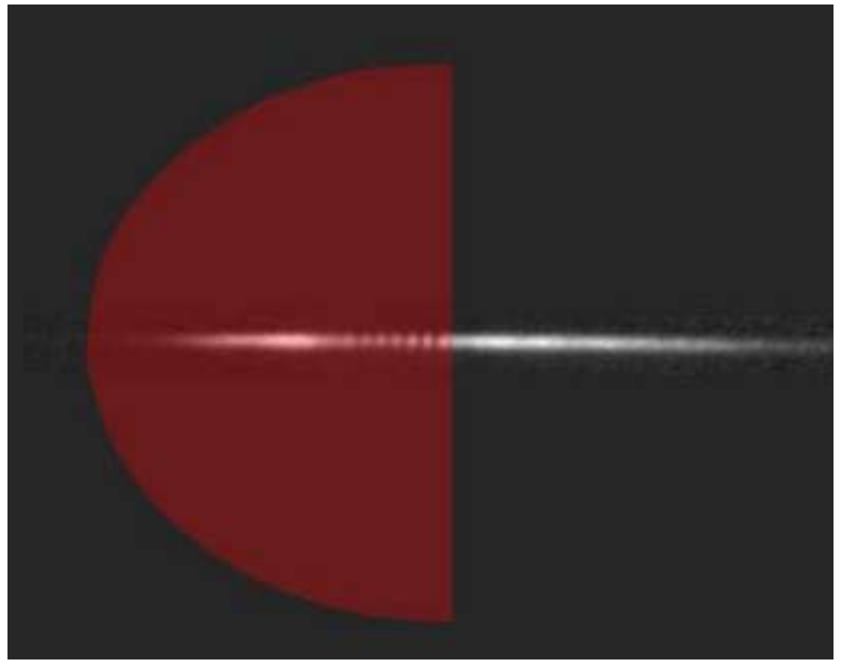

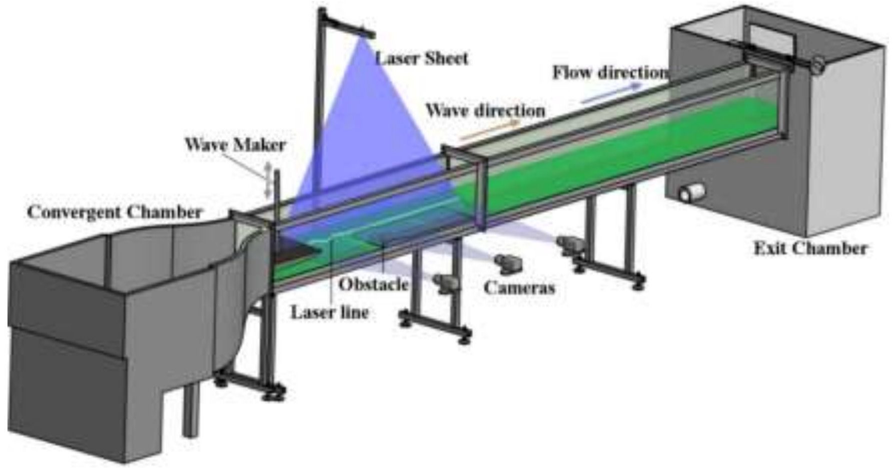

Euve', L.P. *et al*, *PRL*, **124**, 141101 (2020)

Guerrero, K. *et al*, *PRL*, **135**, 243801 (2025)

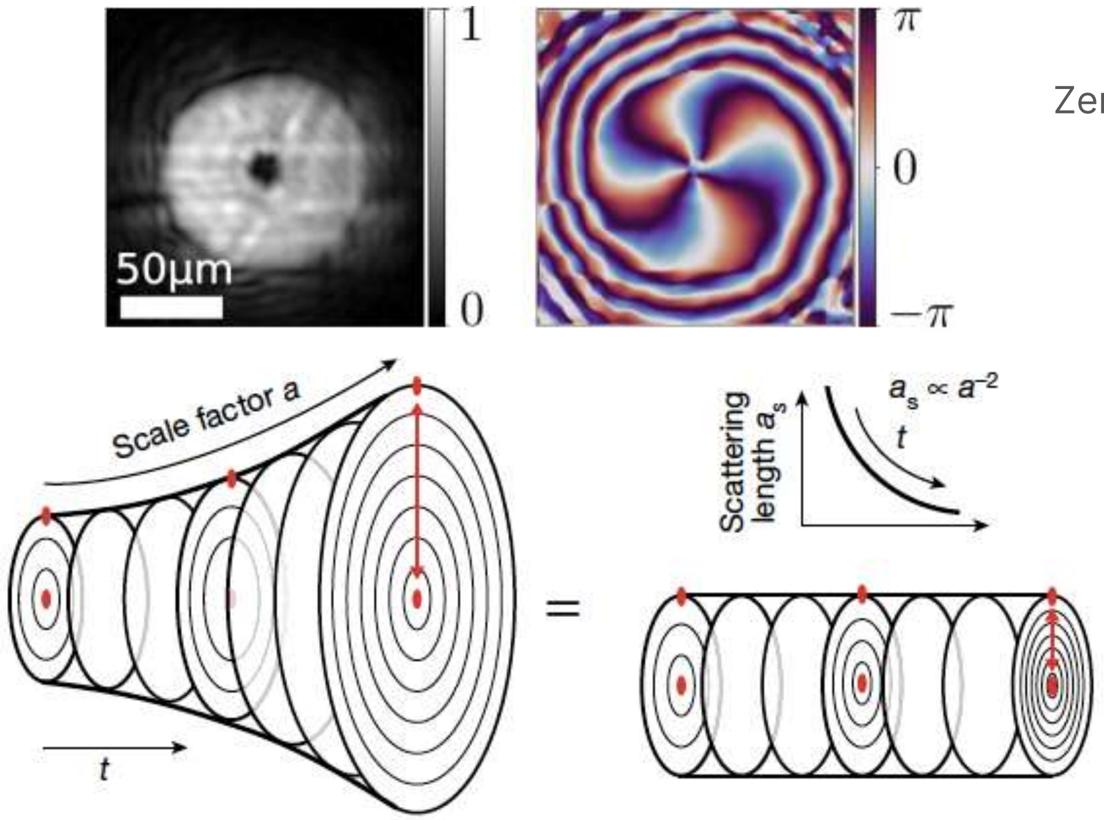

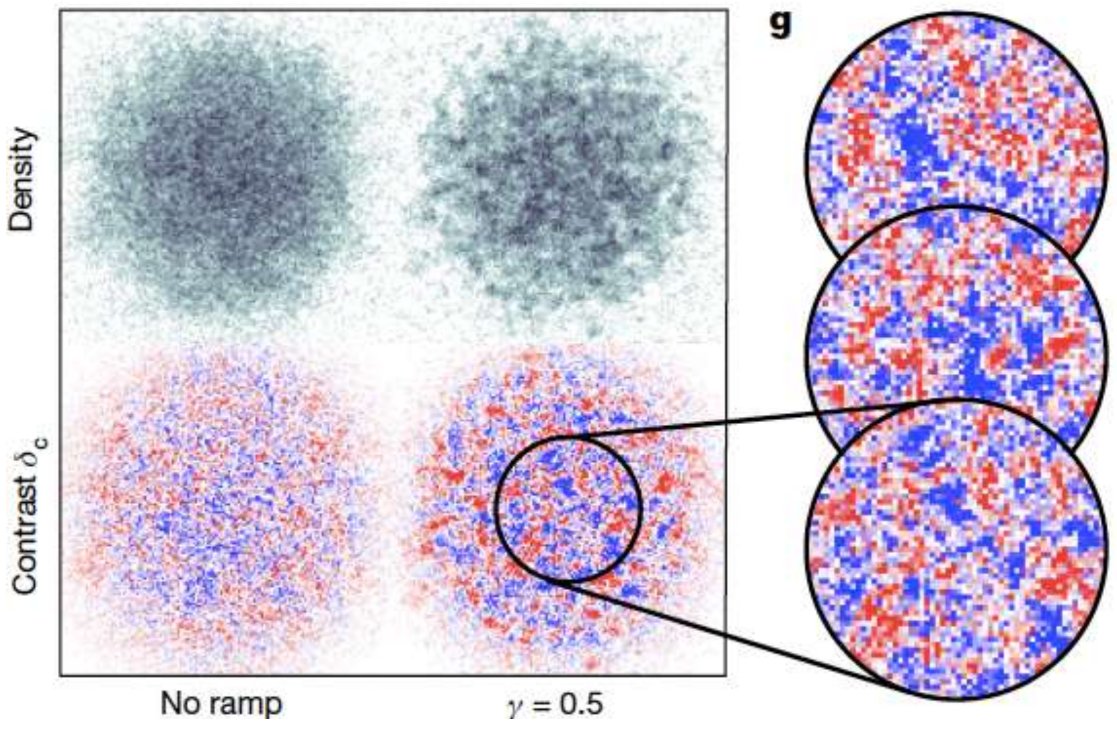

Viermann, C. et al, *Nature*, **611**, 260–264 (2022)

Zenesini, A. *et al*, *Nat. Phys.*, **20**, 558–563 (2024)

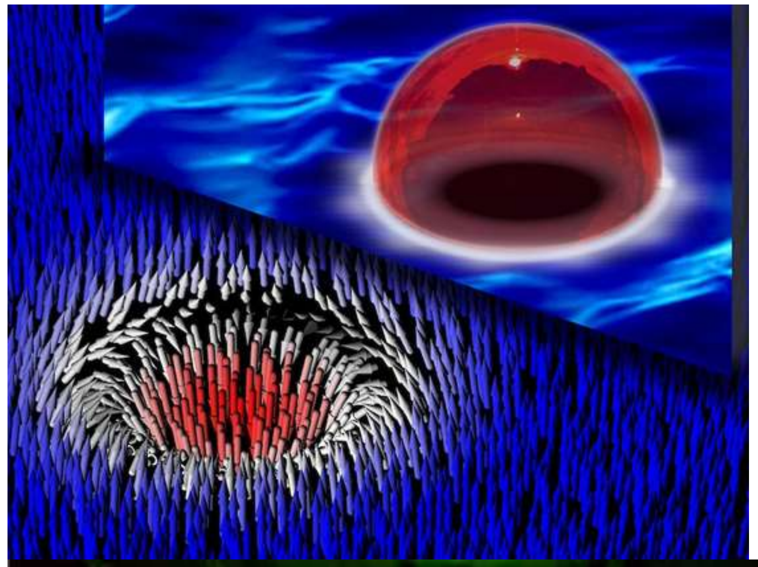

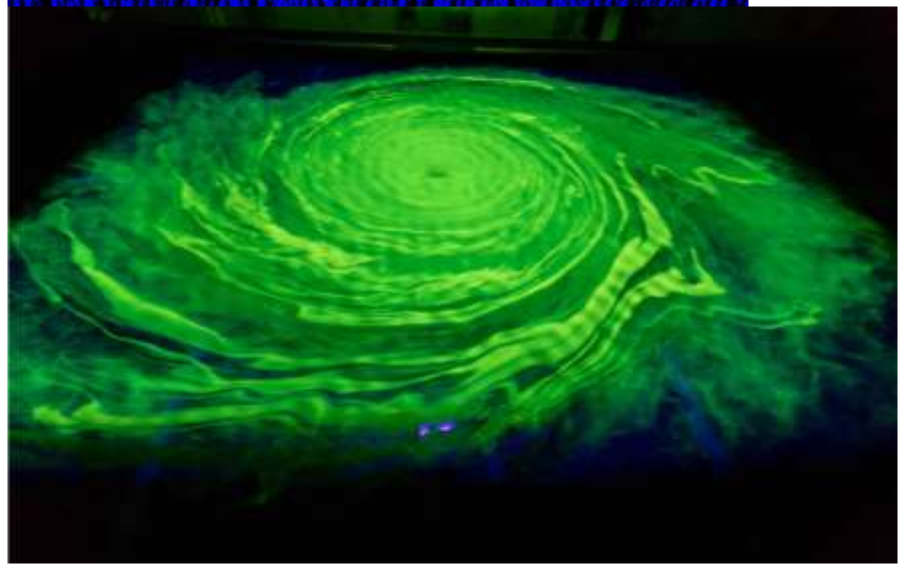

Torres, T. *et al*, *Nat. Phys.*, **13**, 833–836 (2017)

Techniques and Motivations

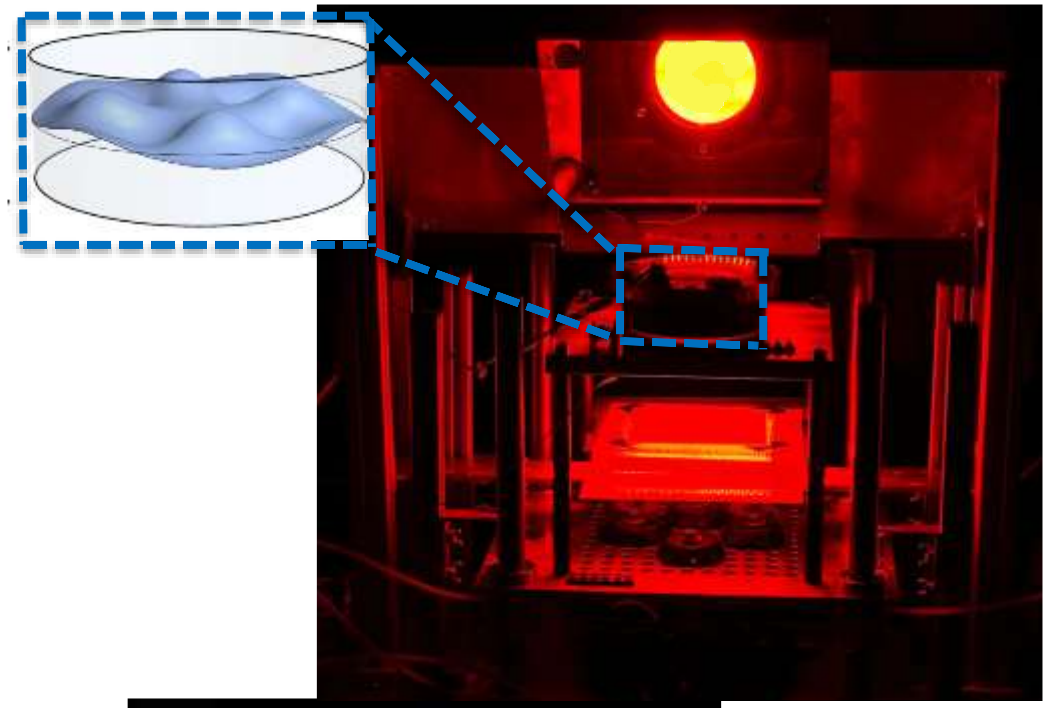

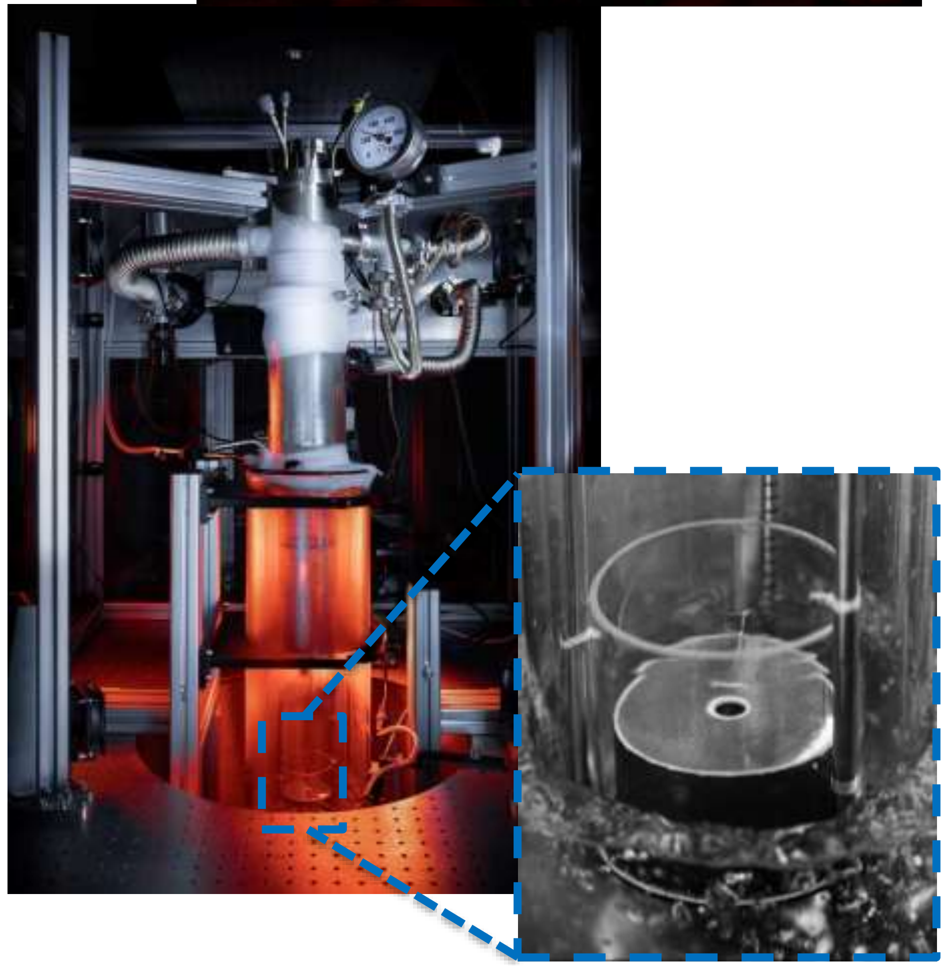

Emergence of nonlinear interactions

Schlieren profilometry: high-resolution measurements of the **entire evolution of modes** for each run

Analysis of the **intermediate regime** between well-known steady states common to many field theories

Learn about **relevant wave-mixing processes** taking place at the origins of the fully out-of-equilibrium stage

Connection to a **wide range of driven systems** with highly occupied, interacting modes (→ e.g. cosmological preheating)

Classical fluid dynamical simulator for preheating

Primary instability: *one* mode

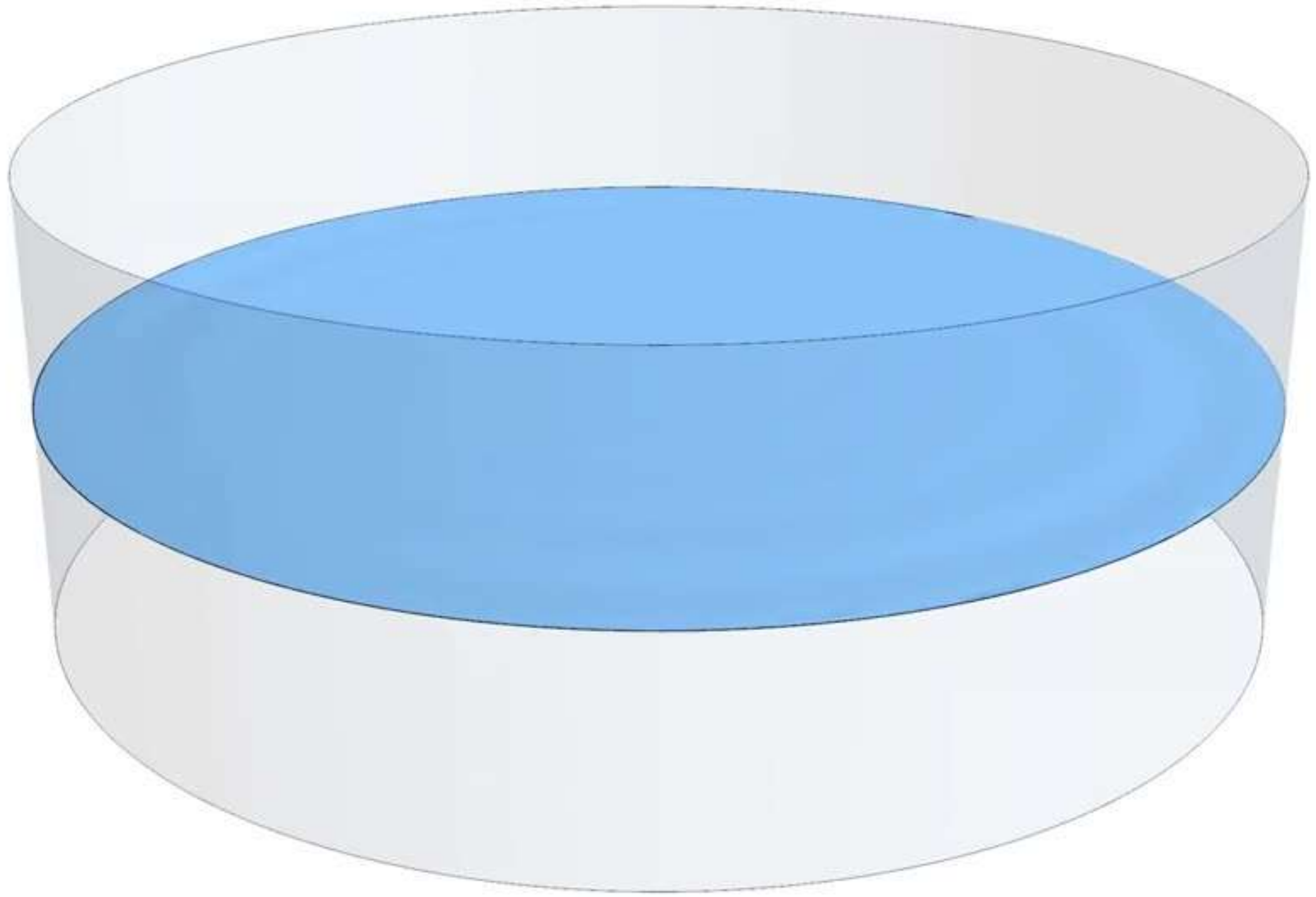

FARADAY PRESCRIPTION

$$\omega_d = 2\omega_0$$

Height field decomposition:

$$\xi(t, r, \theta) \propto \sum_a \underbrace{\xi_a(t)}_{\text{temporal evolution}} \underbrace{R_a(r) e^{i m_a \theta}}_{\text{spatial eigenfunctons}}$$

Cylindrical Bessel functions:

$$\begin{cases} R_{mn}(r) \propto J_m(k_{mn} r) \\ J'_m(k_{mn} r_0) = 0 \end{cases}$$

DOMINANT MODE: $(4, 1)_{\omega_0}$

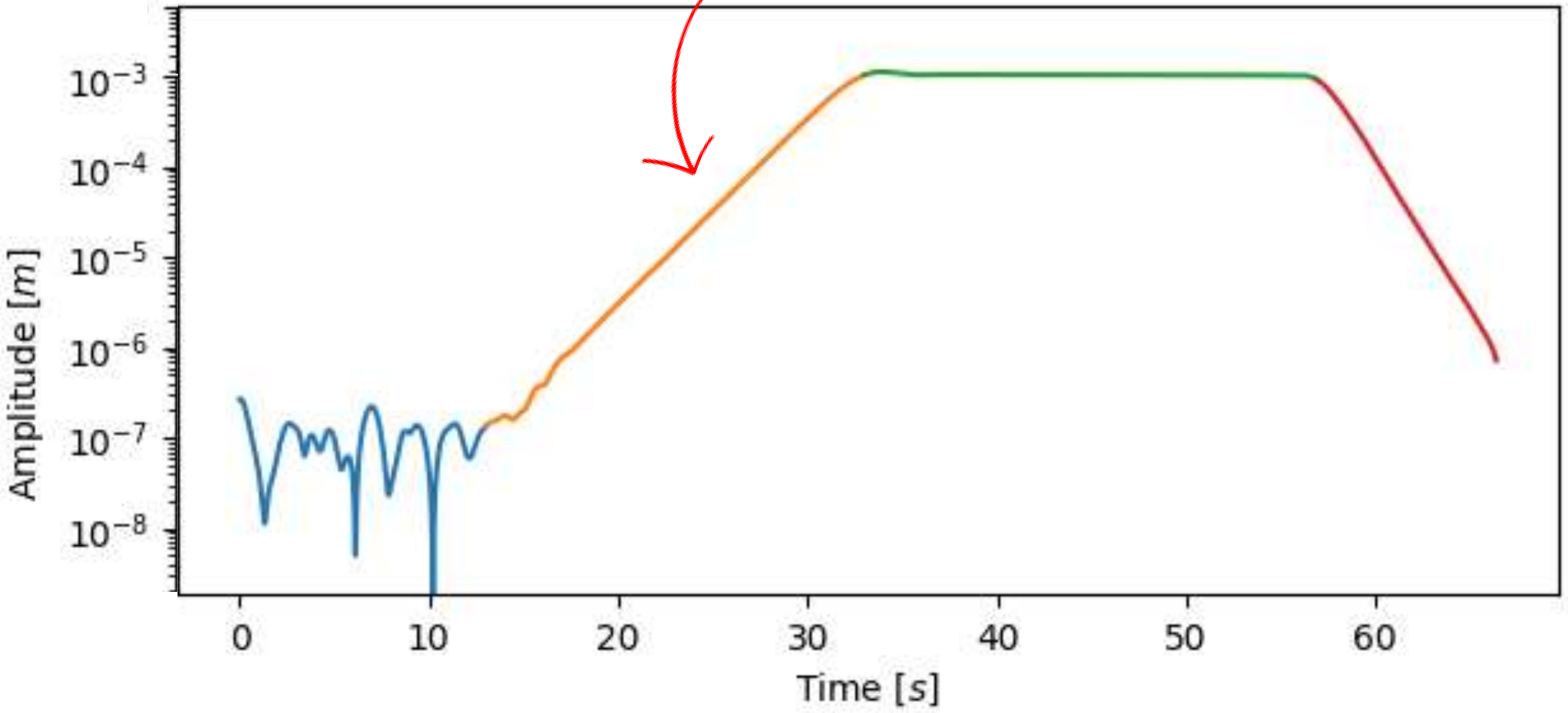

Secondary instabilities: from *few* to *many*

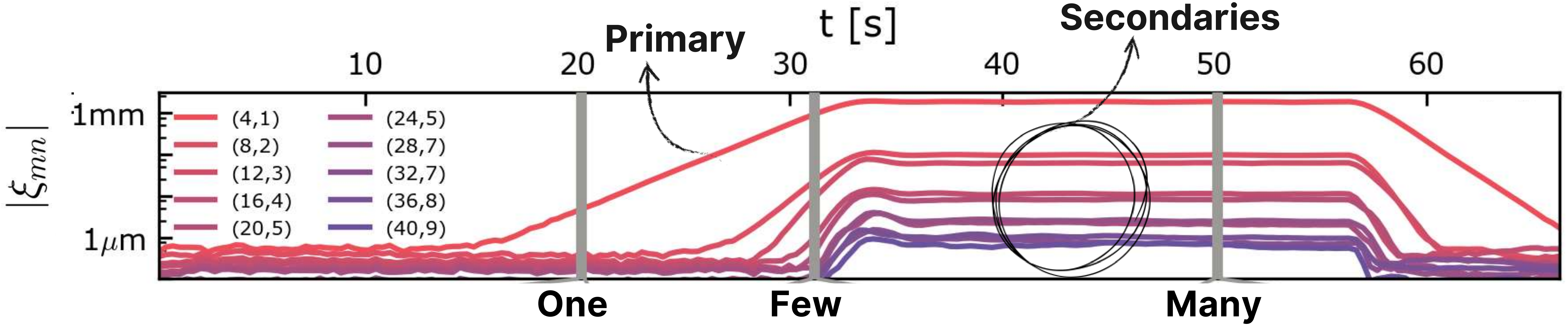

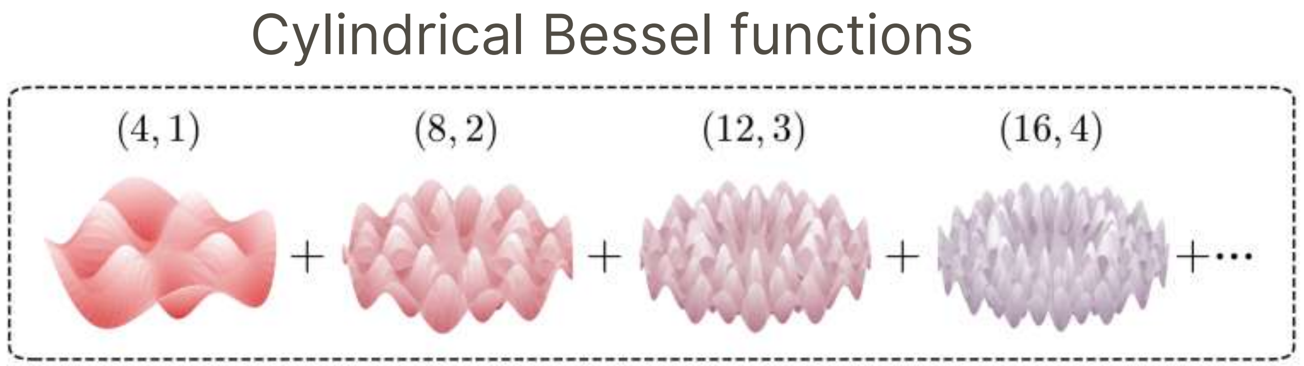

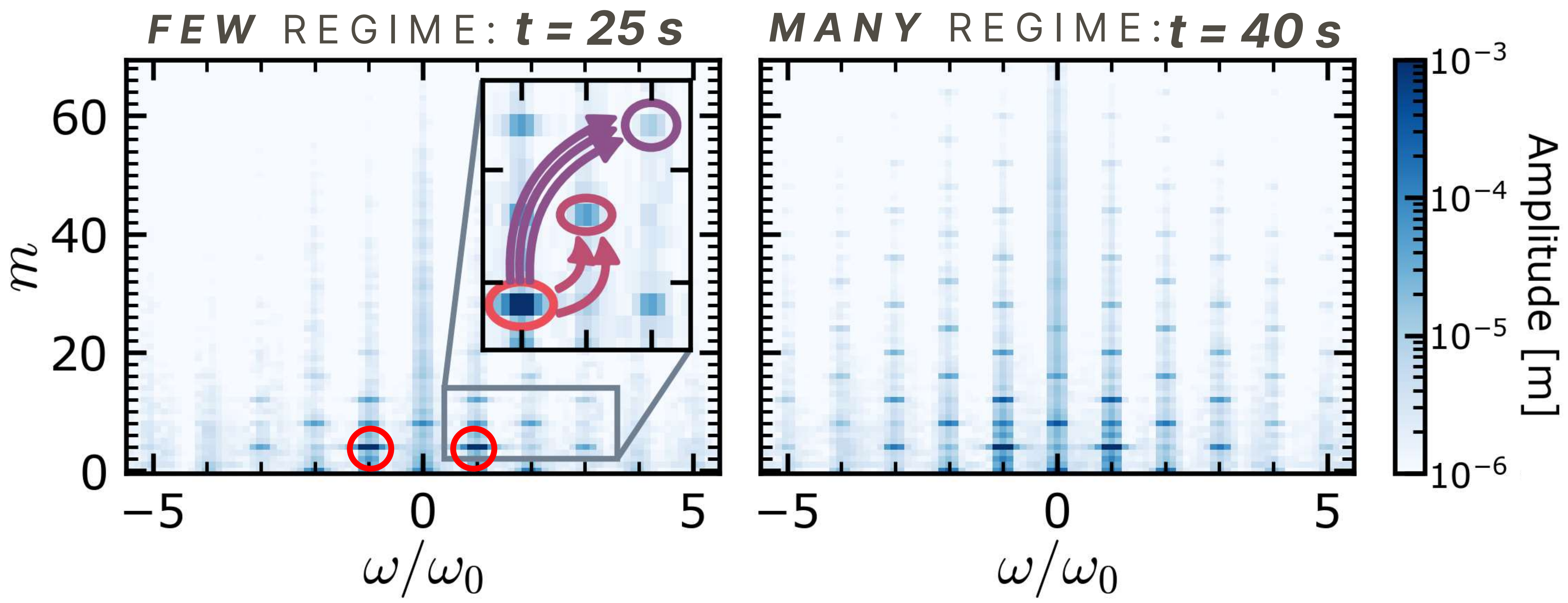

Lagrangian description

Fluids densities

Drive-dependent oscillation

Time-derivative

$$\frac{L}{\Sigma} = \frac{1}{2}\sum_a \frac{\rho_1+\rho_2}{k_a\tanh(k_a h_0)}\left(\dot{\xi}_a^2 - \omega_a^2(t)\xi_a^2\right) + \frac{1}{2}\sum_{a,b,c}(\rho_1-\rho_2)\mathcal{A}_{cab}\xi_c\dot{\xi}_a\dot{\xi}_b$$

$$+\frac{1}{4}\sum_{a,b,c,d}\left[(\rho_1+\rho_2)\mathcal{A}_{cdab}\dot{\xi}_a\dot{\xi}_b + \frac{\sigma}{2}\mathcal{B}_{abcd}\xi_a\xi_b\right]\xi_c\xi_d + \dots$$

Mode momentum

Surface tension

= parametric evolution

= cubic interactions

= quartic interactions

= higher order terms

Silveira, V. B. *et al*, *arXiv:2207.02199*

Silveira, V. B. *et al*, *J. Phys. Conf. Ser.*, **2531** 012003 (2023)

Scattering scheme

Conservation of momentum

$$\frac{L}{\Sigma} = \frac{1}{2}\sum_a \frac{\rho_1+\rho_2}{k_a \tanh(k_a h_0)}\left(\dot{\xi}_a^2 - \omega_a^2(t)\xi_a^2\right) + \frac{1}{2}\sum_{a,b,c}(\rho_1-\rho_2)\mathcal{A}_{cab}\xi_c\dot{\xi}_a\dot{\xi}_b + \frac{1}{4}\sum_{a,b,c,d}\left[(\rho_1+\rho_2)\mathcal{A}_{cdab}\dot{\xi}_a\dot{\xi}_b + \frac{\sigma}{2}\mathcal{B}_{abcd}\xi_a\xi_b\right]\xi_c\xi_d$$

$$\mathcal{A}_{cab} \propto \delta_{m_c,\pm|m_a\pm m_b|},$$
$$\mathcal{A}_{cdab}, \mathcal{B}_{cdab} \propto \delta_{\pm m_c \pm m_d, \pm m_a \pm m_b}$$

Cubic scattering scheme

$$(4,1)_{\omega_0} + (4,1)_{\omega_0} \rightarrow (8,2)_{2\omega_0}$$

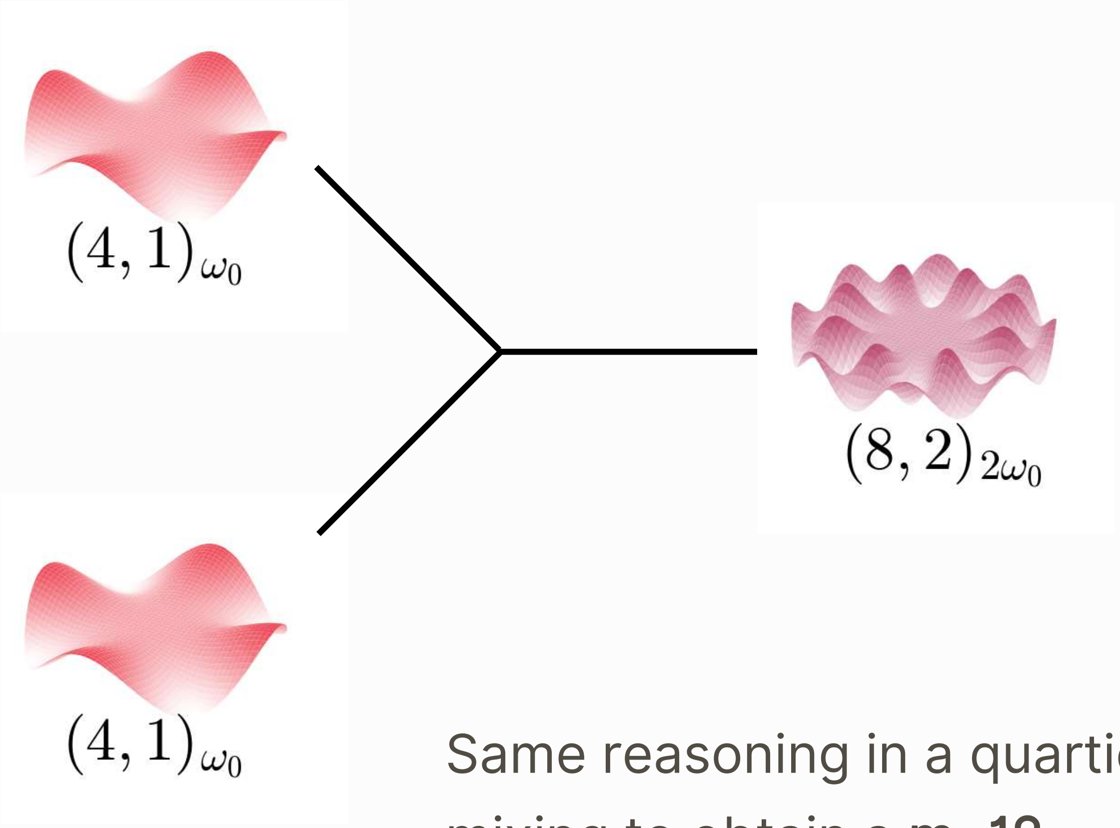

Same reasoning in a quartic mixing to obtain a **m=12**

Time correlation functions: *few* modes

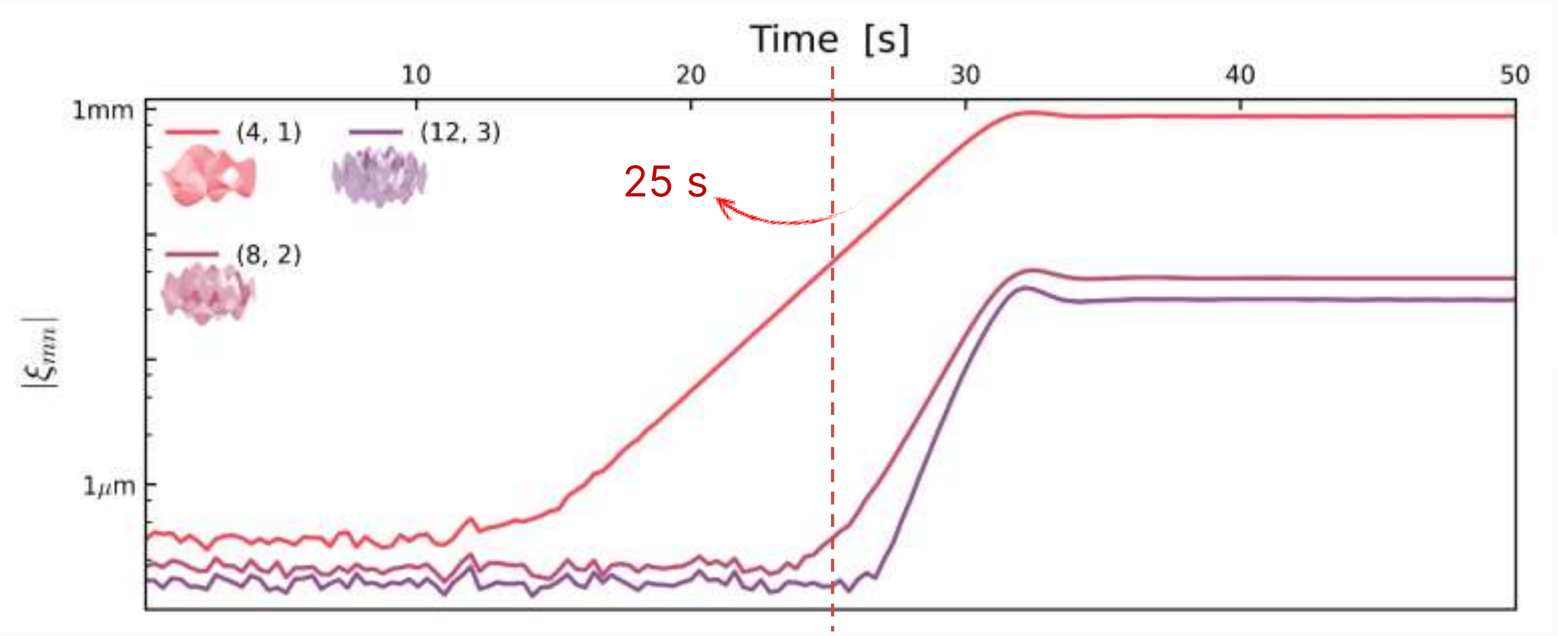

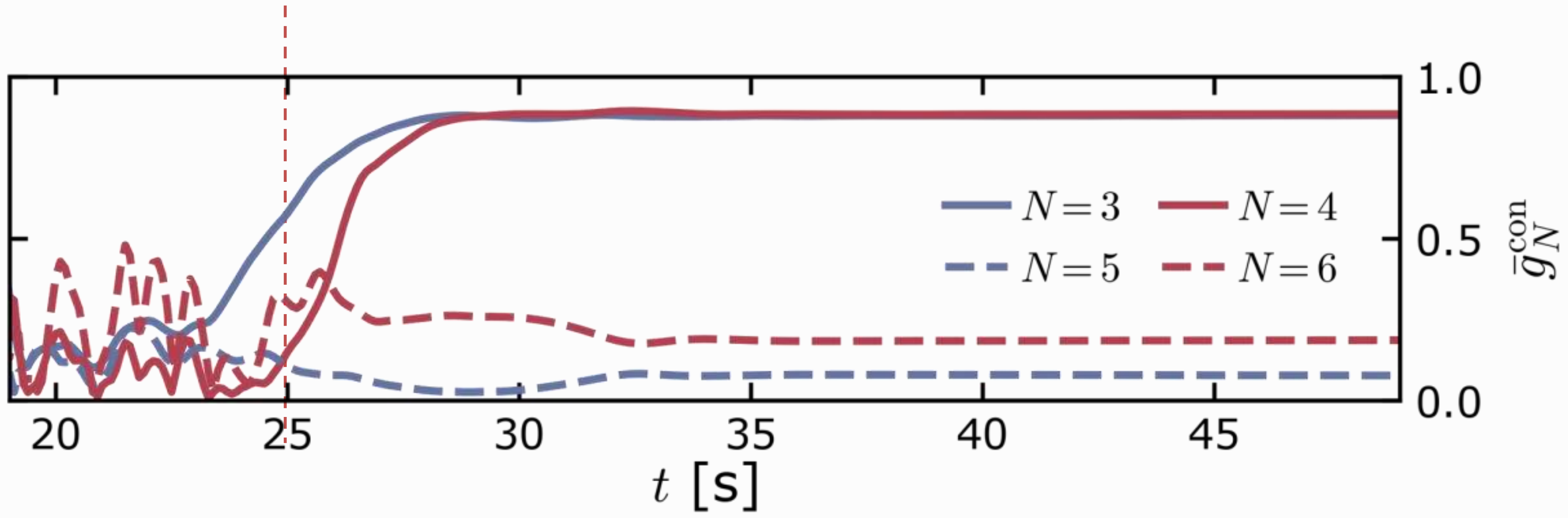

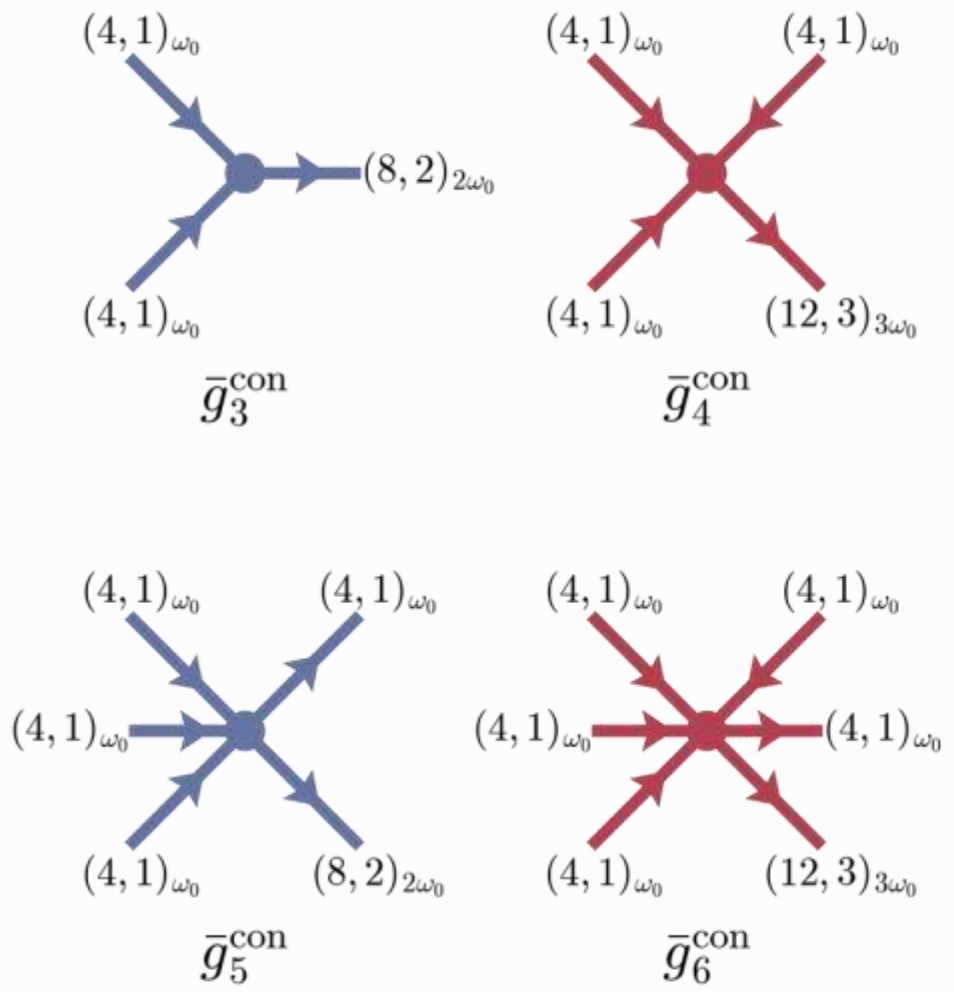

Correlation functions for $\xi_i \equiv \xi_{m_i,\omega_i}$

$$g_N(\xi_1 \ldots \xi_N) = \langle \xi_1 \ldots \xi_N \rangle$$

g_N averaged over experimental runs, r, θ ⟶ $\bar{g}_N(t) \equiv \frac{|\langle \xi_1 \ldots \xi_N \rangle_c|}{\langle |\xi_1 \ldots \xi_N| \rangle}$

Schweigler, T. *et al*, *Nature*, **545**, 323 (2017)

Time correlation functions: *few* modes

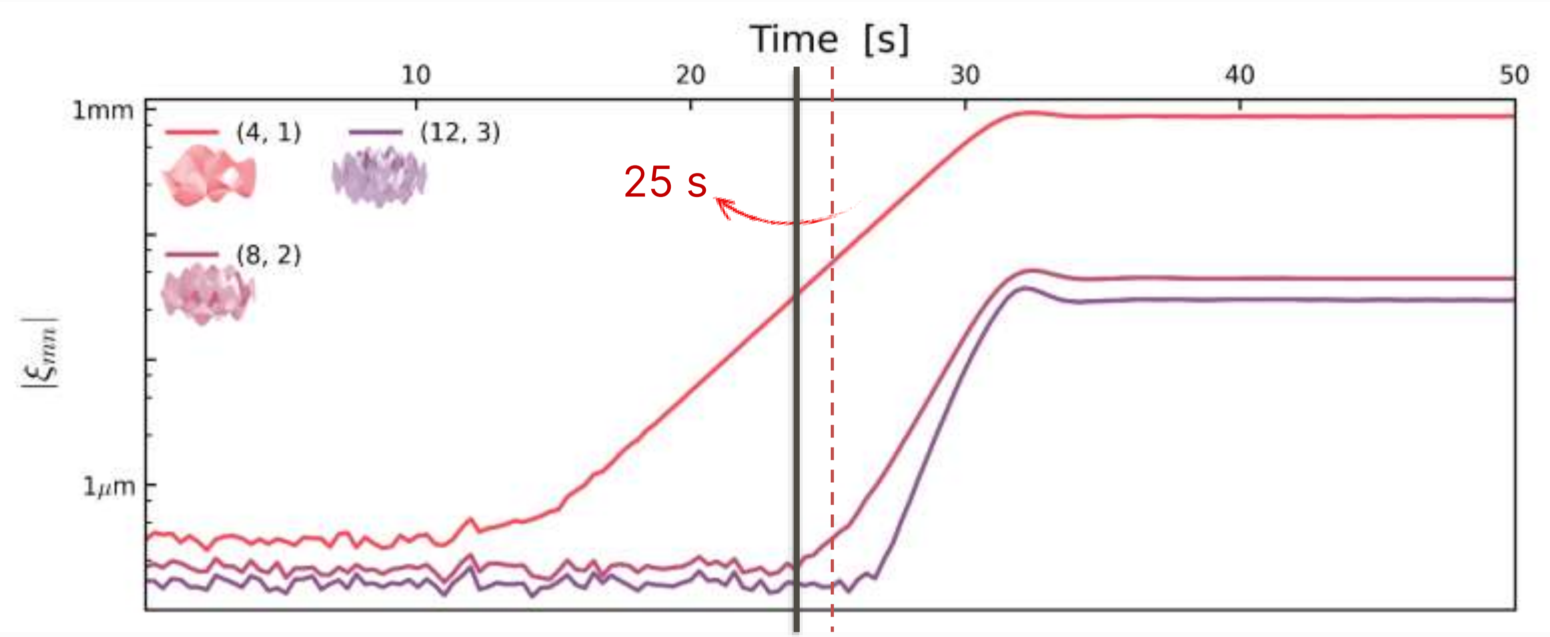

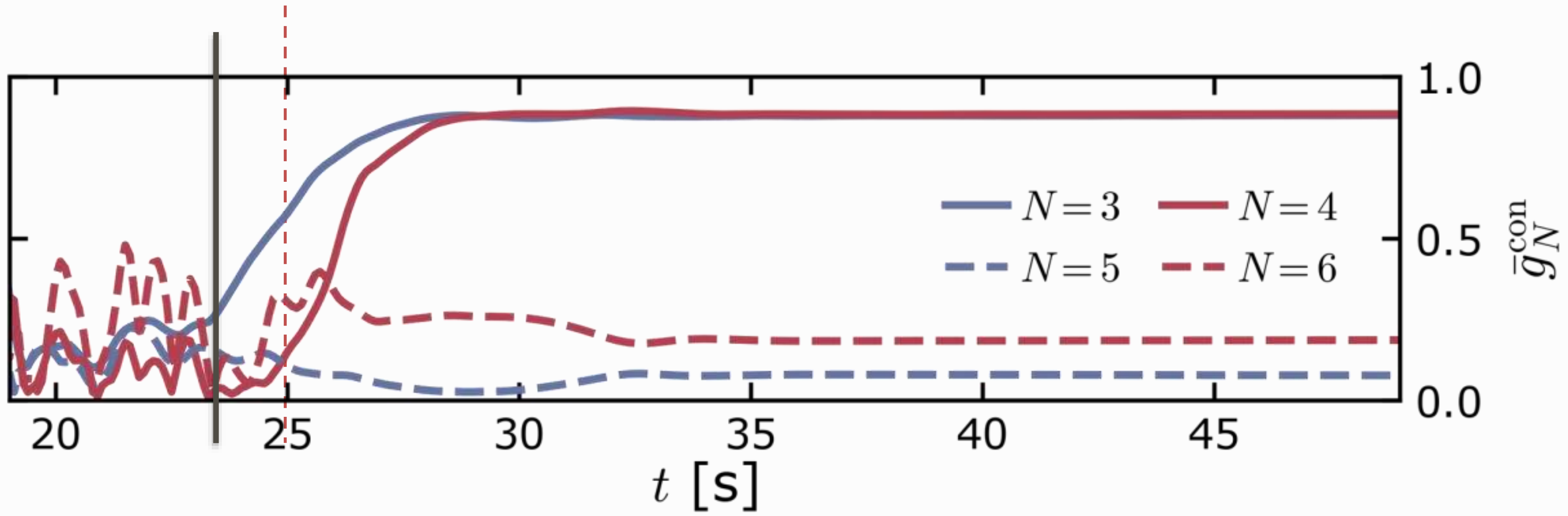

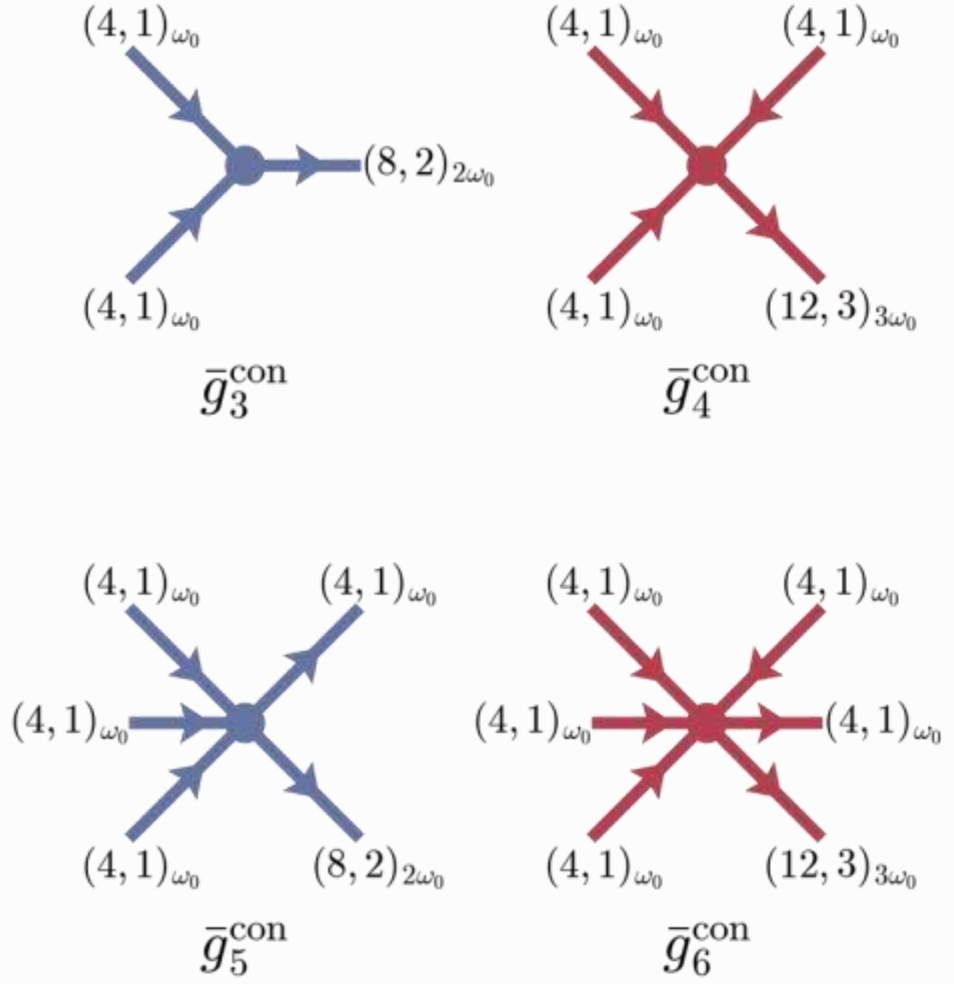

Correlation functions for $\xi_i \equiv \xi_{m_i,\omega_i}$

$$g_N(\xi_1 \ldots \xi_N) = \langle \xi_1 \ldots \xi_N \rangle$$

g_N averaged over experimental runs, r, θ ⟶ $\bar{g}_N(t) \equiv \frac{|\langle \xi_1 \ldots \xi_N \rangle_c|}{\langle |\xi_1 \ldots \xi_N| \rangle}$

Schweigler, T. *et al*, *Nature*, **545**, 323 (2017)

Time correlation functions: *few* modes

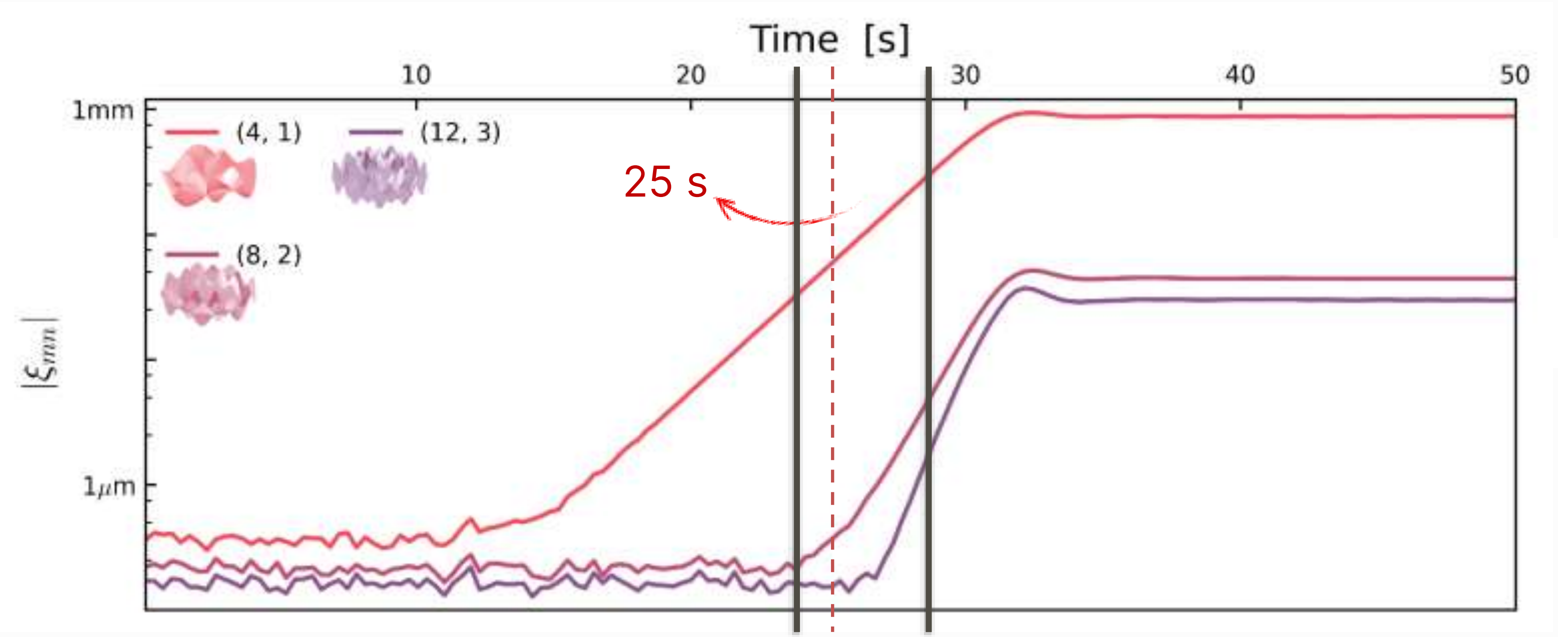

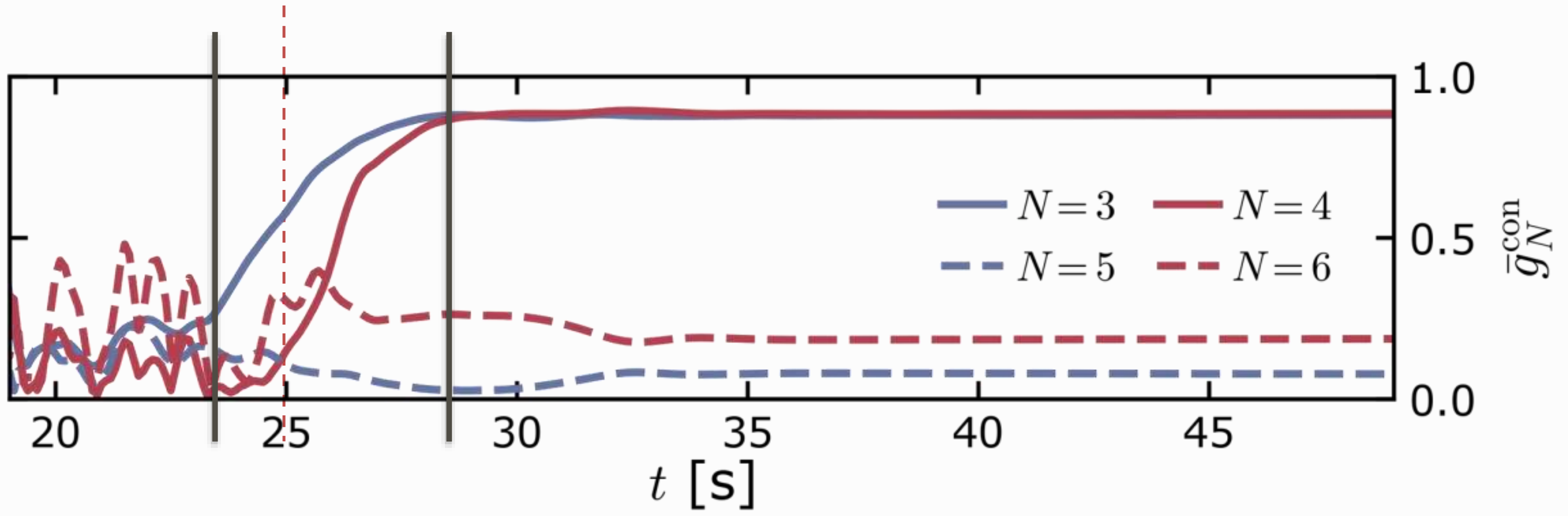

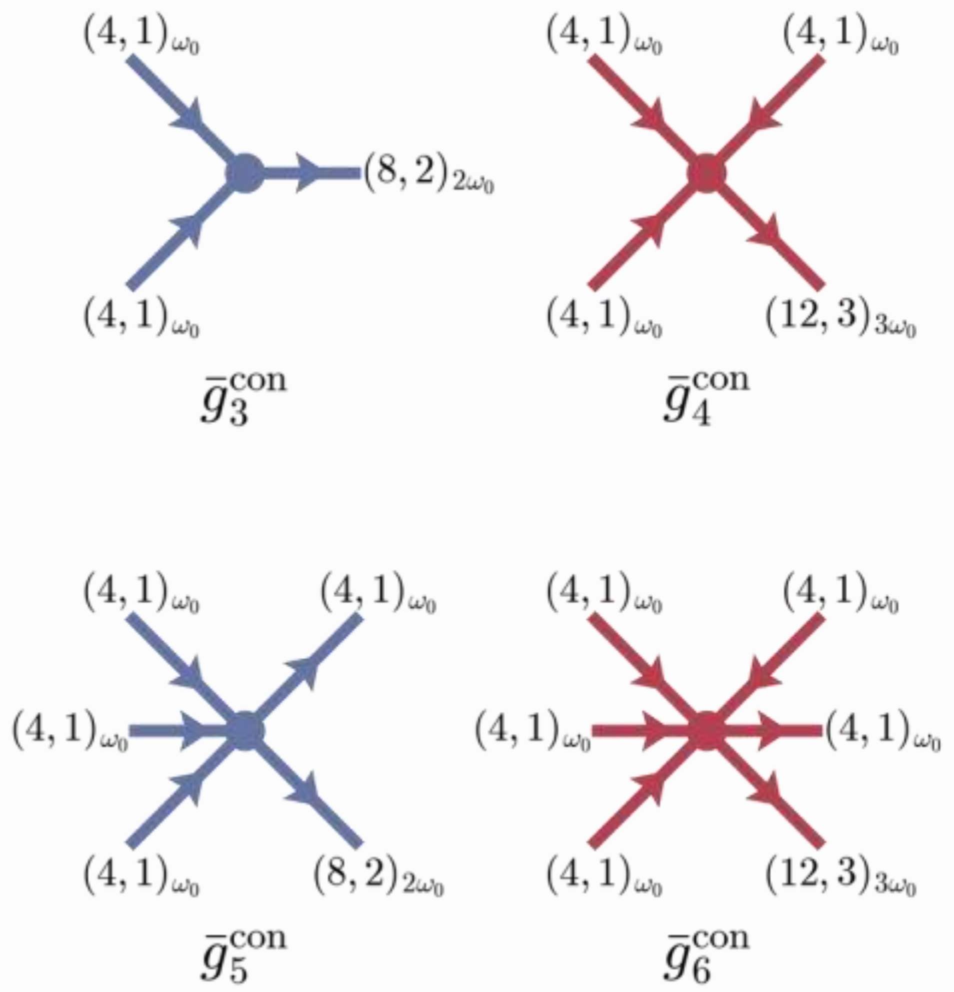

Correlation functions for $\xi_i \equiv \xi_{m_i,\omega_i}$

$$g_N(\xi_1 \ldots \xi_N) = \langle \xi_1 \ldots \xi_N \rangle$$

g_N averaged over experimental runs, r, θ ⟶ $\bar{g}_N(t) \equiv \dfrac{|\langle \xi_1 \ldots \xi_N \rangle_c|}{\langle |\xi_1 \ldots \xi_N| \rangle}$

Schweigler, T. *et al*, *Nature*, **545**, 323 (2017)

Frequency correlation functions: *many* modes

Correlation functions

$$G_N(\omega_1, \ldots, \omega_N) = \langle \xi_{\omega_1} \ldots \xi_{\omega_N} \rangle$$

$$G_N(\omega_1, \ldots, \omega_N) = \sum_{m_1,\ldots,m_N} g_N(\xi_{m_1,\omega_1} \ldots \xi_{m_N,\omega_N})$$

G_N averaged over experimental runs, t, r, θ:

$$\bar{G}_N(\omega_1, \ldots, \omega_N) = \frac{|\langle \xi_{\omega_1} \ldots \xi_{\omega_N} \rangle_c|}{\langle |\xi_{\omega_1} \ldots \xi_{\omega_N}| \rangle}$$

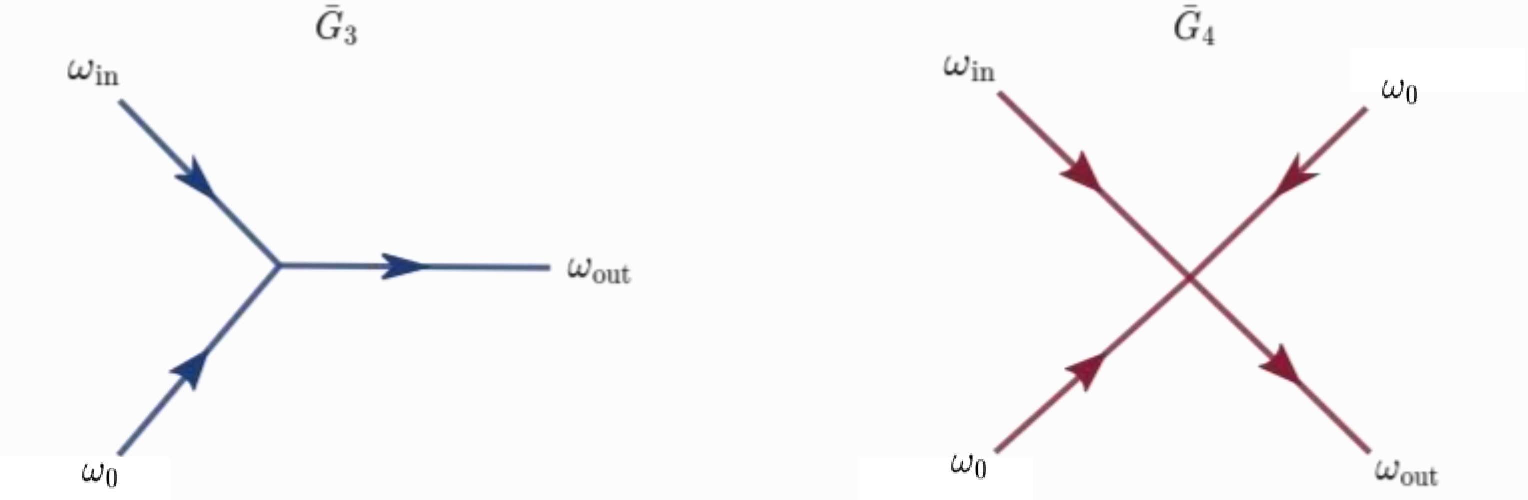

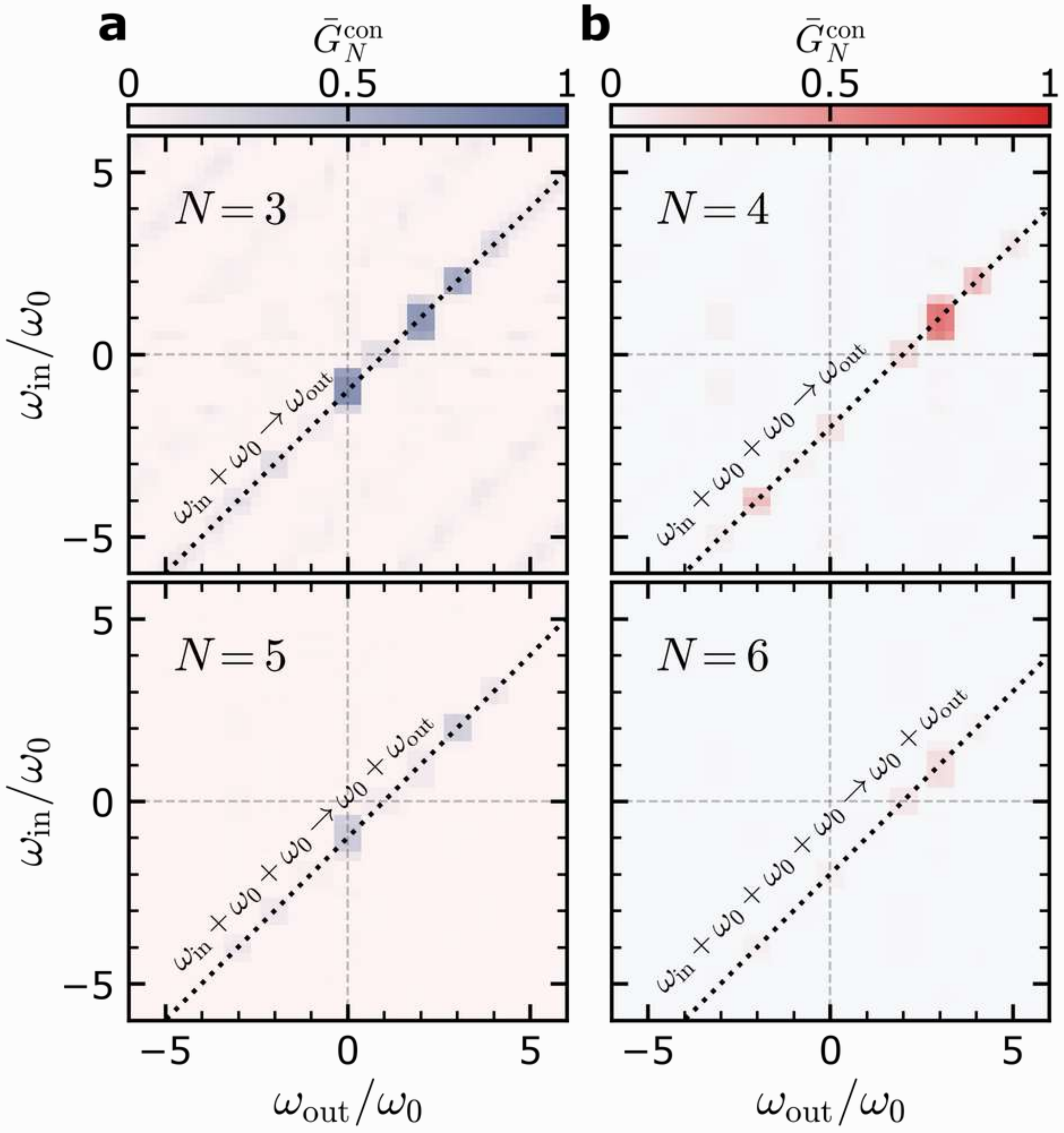

Frequency correlation functions: *many* modes

Correlation functions

$$G_N(\omega_1, \ldots, \omega_N) = \langle \xi_{\omega_1} \ldots \xi_{\omega_N} \rangle$$

G_N averaged over experimental runs, t, r, θ:

$$\bar{G}_N(\omega_1, \ldots, \omega_N) = \frac{|\langle \xi_{\omega_1} \ldots \xi_{\omega_N} \rangle_c|}{\langle |\xi_{\omega_1} \ldots \xi_{\omega_N}| \rangle}$$

Examples

$$\omega_0 + \omega_0 \rightarrow 2\omega_0$$

$$(4,1)_{\omega_0} + (4,1)_{\omega_0} \rightarrow (8,2)_{2\omega_0}$$

$$\omega_0 + 2\omega_0 \rightarrow 3\omega_0$$

$$(20,n)_{\omega_0} + (16,n')_{2\omega_0} \rightarrow (36,n'')_{3\omega_0}$$

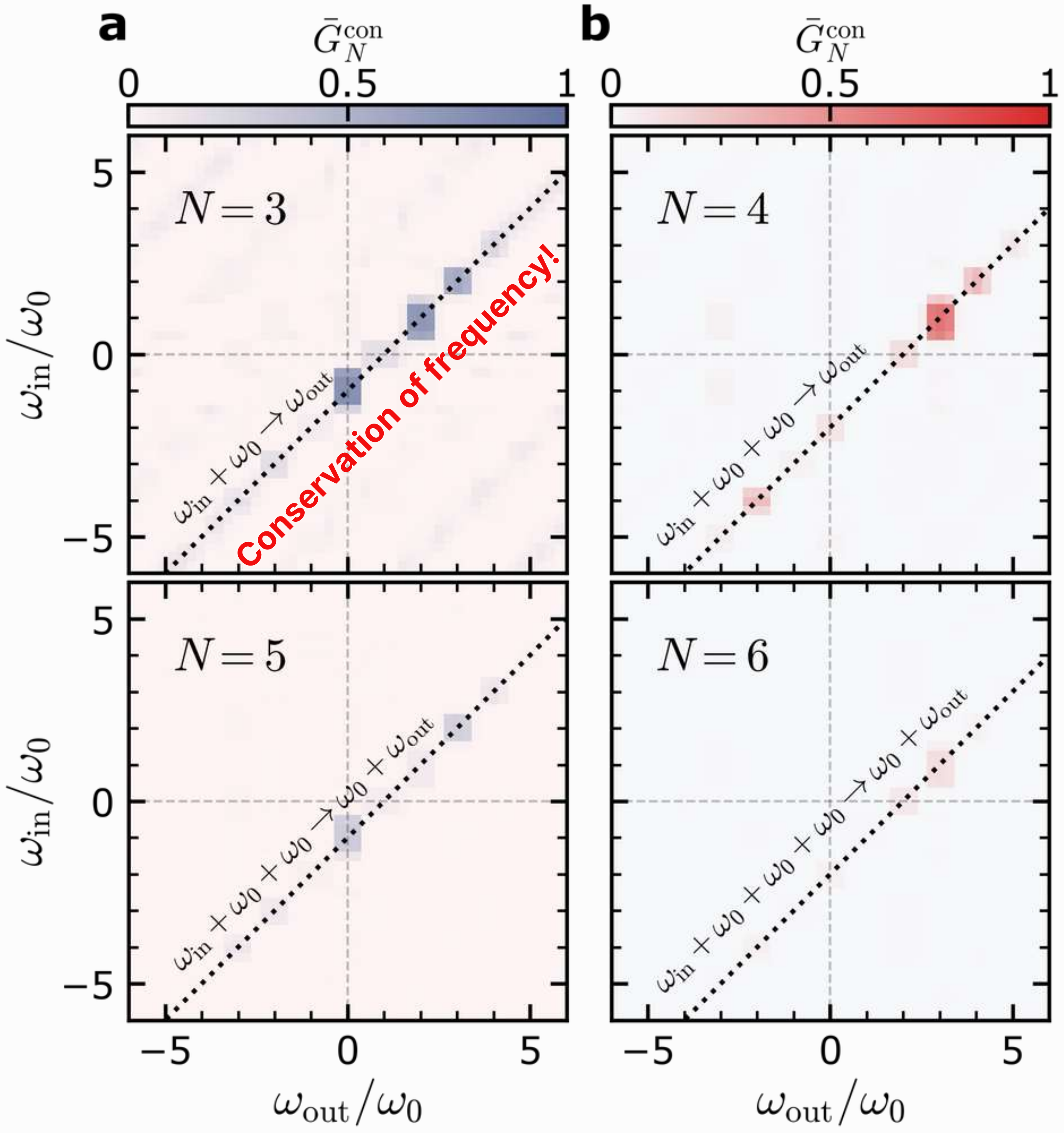

Frequency correlation functions: *many* modes

Correlation functions

$$G_N(\omega_1, \ldots, \omega_N) = \langle \xi_{\omega_1} \ldots \xi_{\omega_N} \rangle$$

G_N averaged over experimental runs, t, r, θ:

$$\bar{G}_N(\omega_1, \ldots, \omega_N) = \frac{|\langle \xi_{\omega_1} \ldots \xi_{\omega_N} \rangle_c|}{\langle |\xi_{\omega_1} \ldots \xi_{\omega_N}| \rangle}$$

Examples

$\omega_0 + \omega_0 \rightarrow 2\omega_0$

$$(4,1)_{\omega_0} + (4,1)_{\omega_0} \rightarrow (8,2)_{2\omega_0}$$

$\omega_0 + 2\omega_0 \rightarrow 3\omega_0$

$$(20,n)_{\omega_0} + (16,n')_{2\omega_0} \rightarrow (36,n'')_{3\omega_0}$$

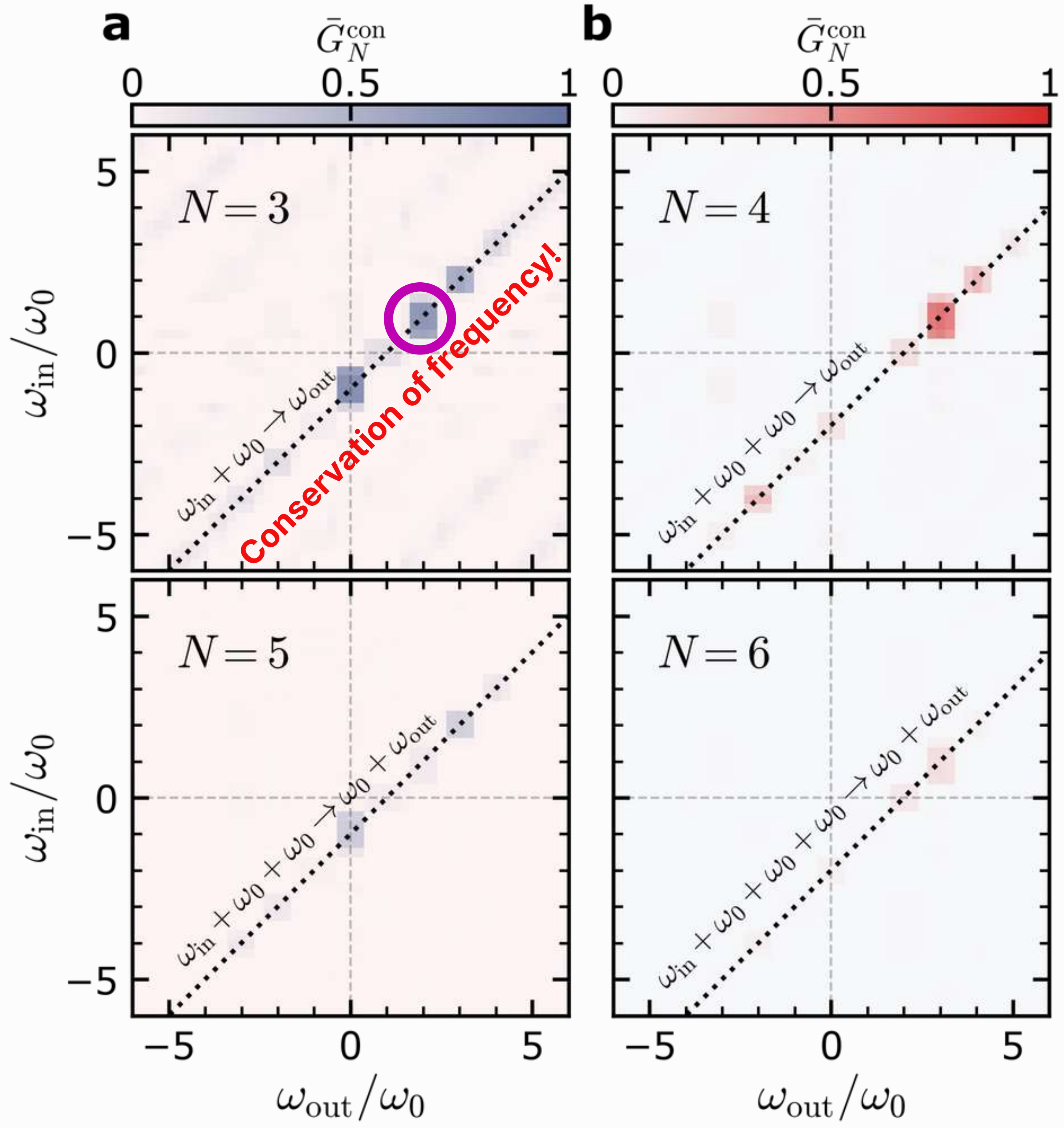

Frequency correlation functions: *many* modes

Correlation functions

$$G_N(\omega_1, \ldots, \omega_N) = \langle \xi_{\omega_1} \ldots \xi_{\omega_N} \rangle$$

G_N averaged over experimental runs, t, r, θ:

$$\bar{G}_N(\omega_1, \ldots, \omega_N) = \frac{|\langle \xi_{\omega_1} \ldots \xi_{\omega_N} \rangle_c|}{\langle |\xi_{\omega_1} \ldots \xi_{\omega_N}| \rangle}$$

Examples

$$\omega_0 + \omega_0 \rightarrow 2\omega_0$$

$$(4,1)_{\omega_0} + (4,1)_{\omega_0} \rightarrow (8,2)_{2\omega_0}$$

$$\omega_0 + 2\omega_0 \rightarrow 3\omega_0$$

$$(20,n)_{\omega_0} + (16,n')_{2\omega_0} \rightarrow (36,n'')_{3\omega_0}$$

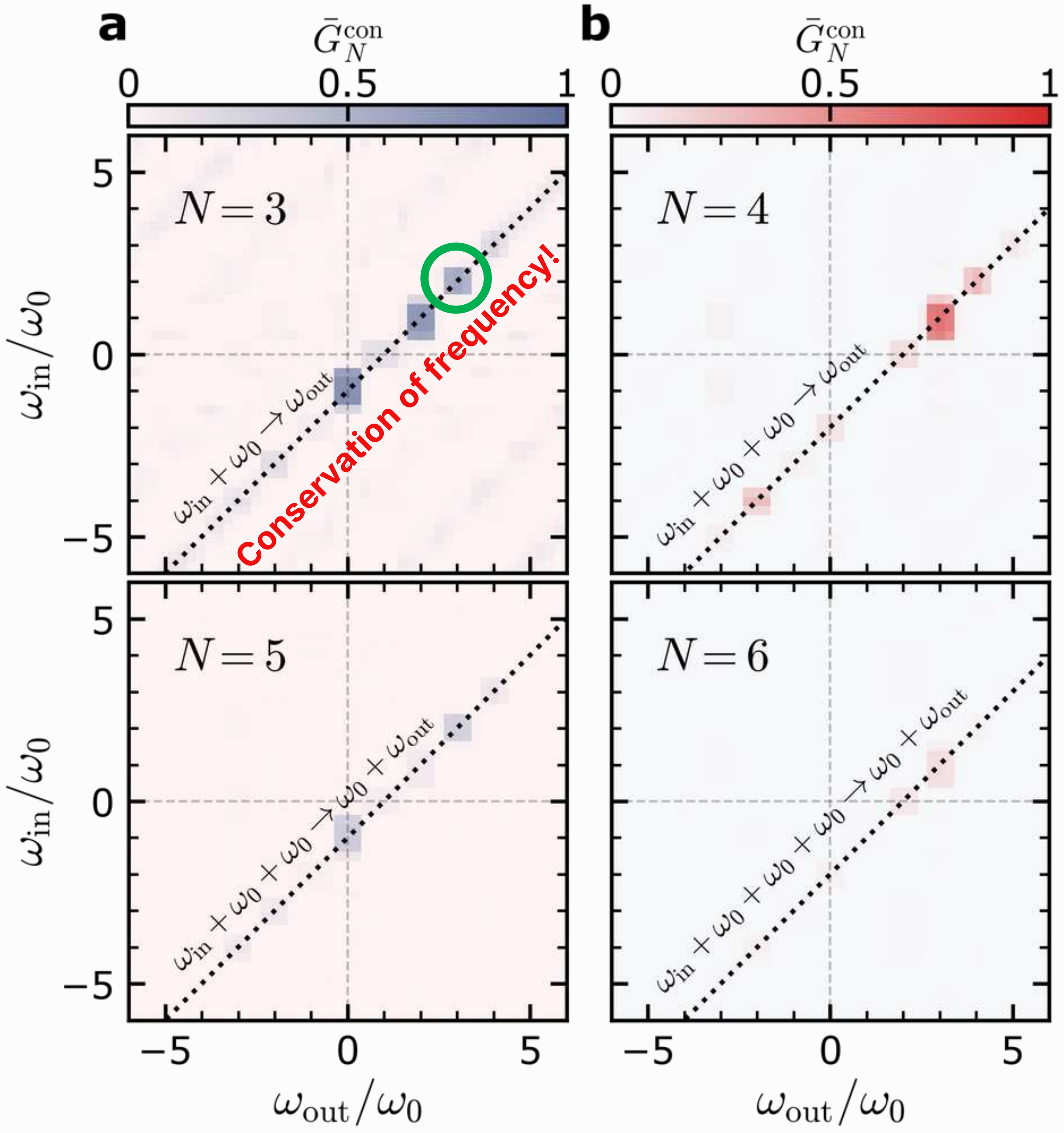

Quantum fluid dynamical simulator for black holes

Sloshing mode

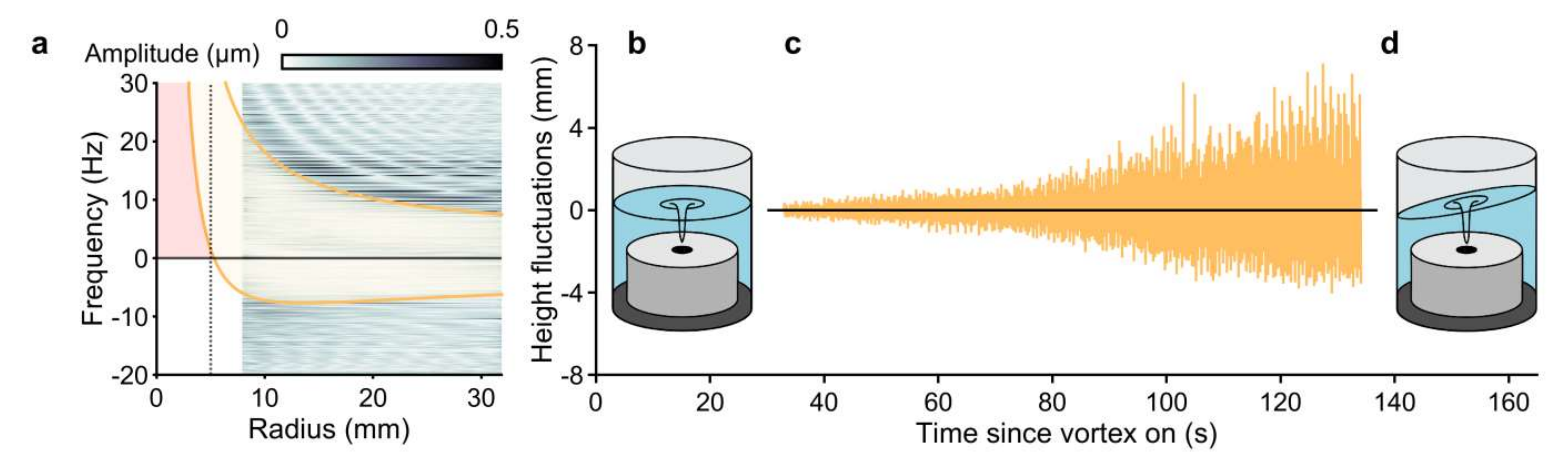

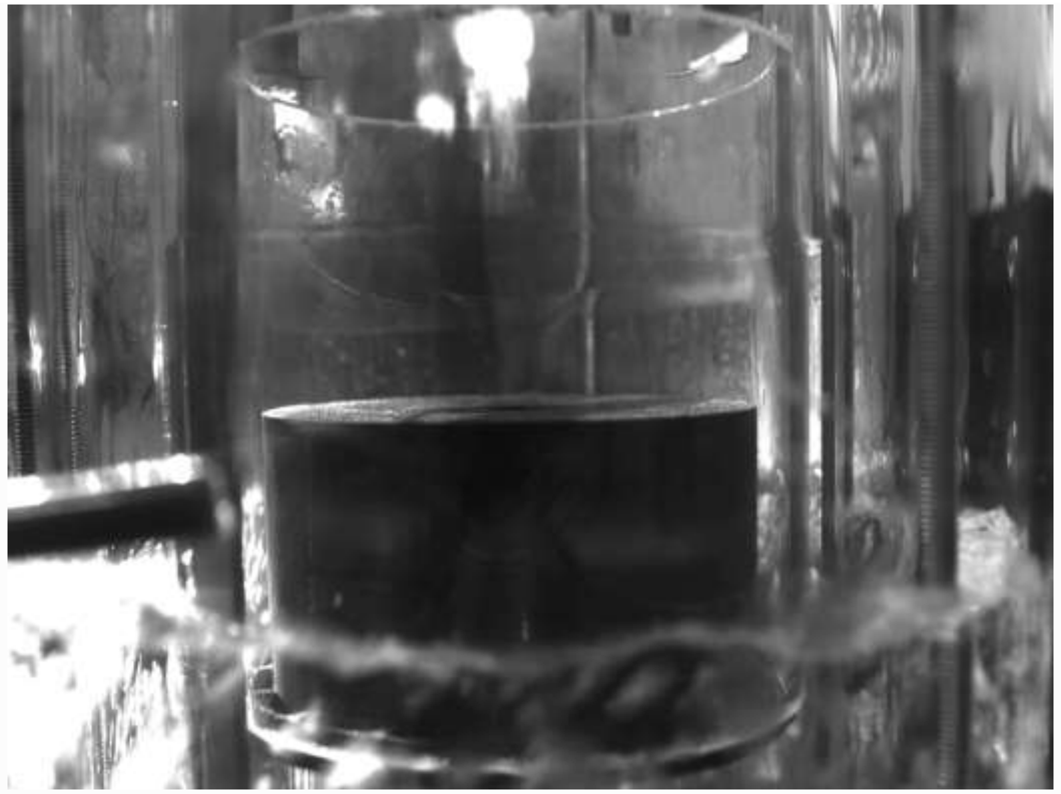

Sloshing mode

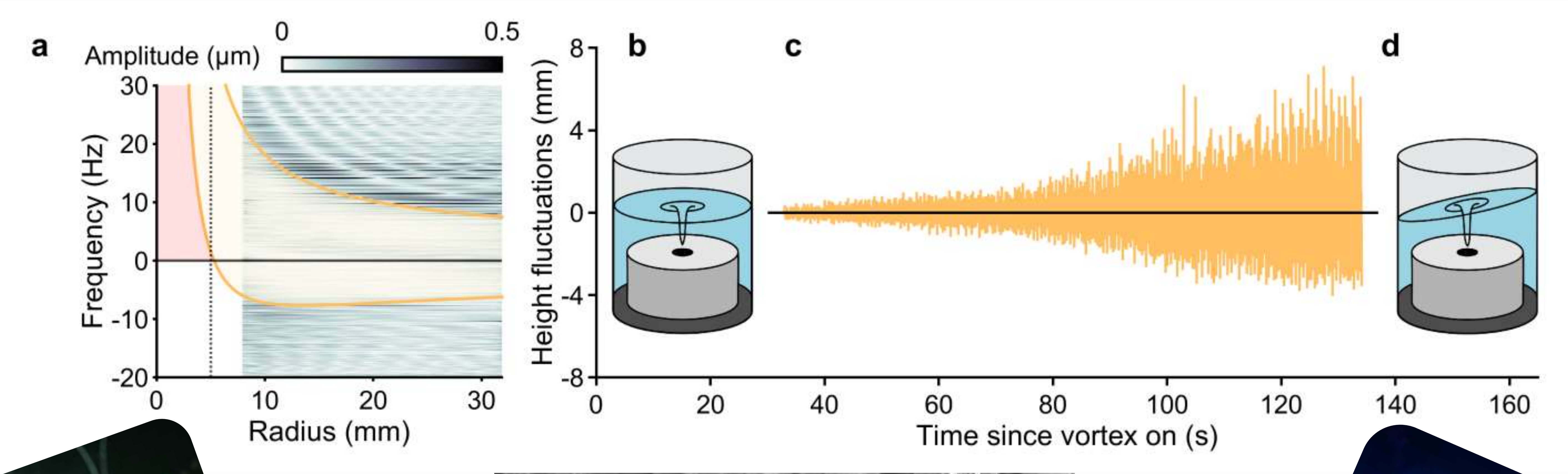

Chris
(experiment)

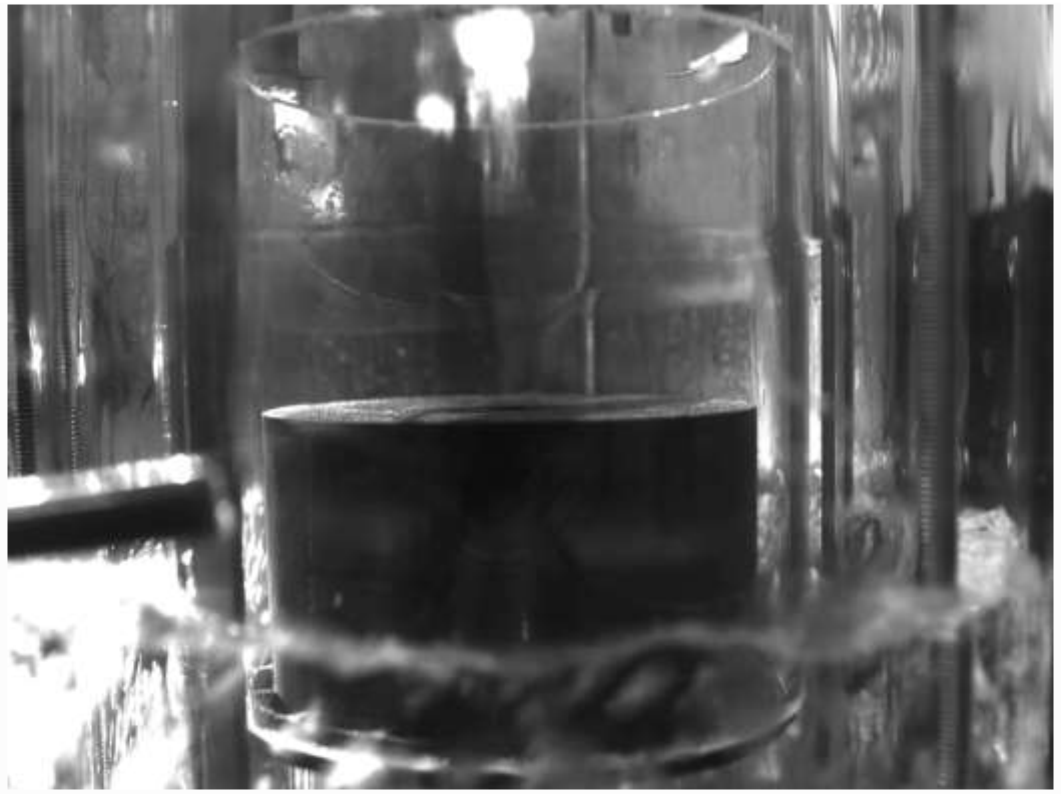

Leonardo
(theory)

Emergence of the nonlinear regime

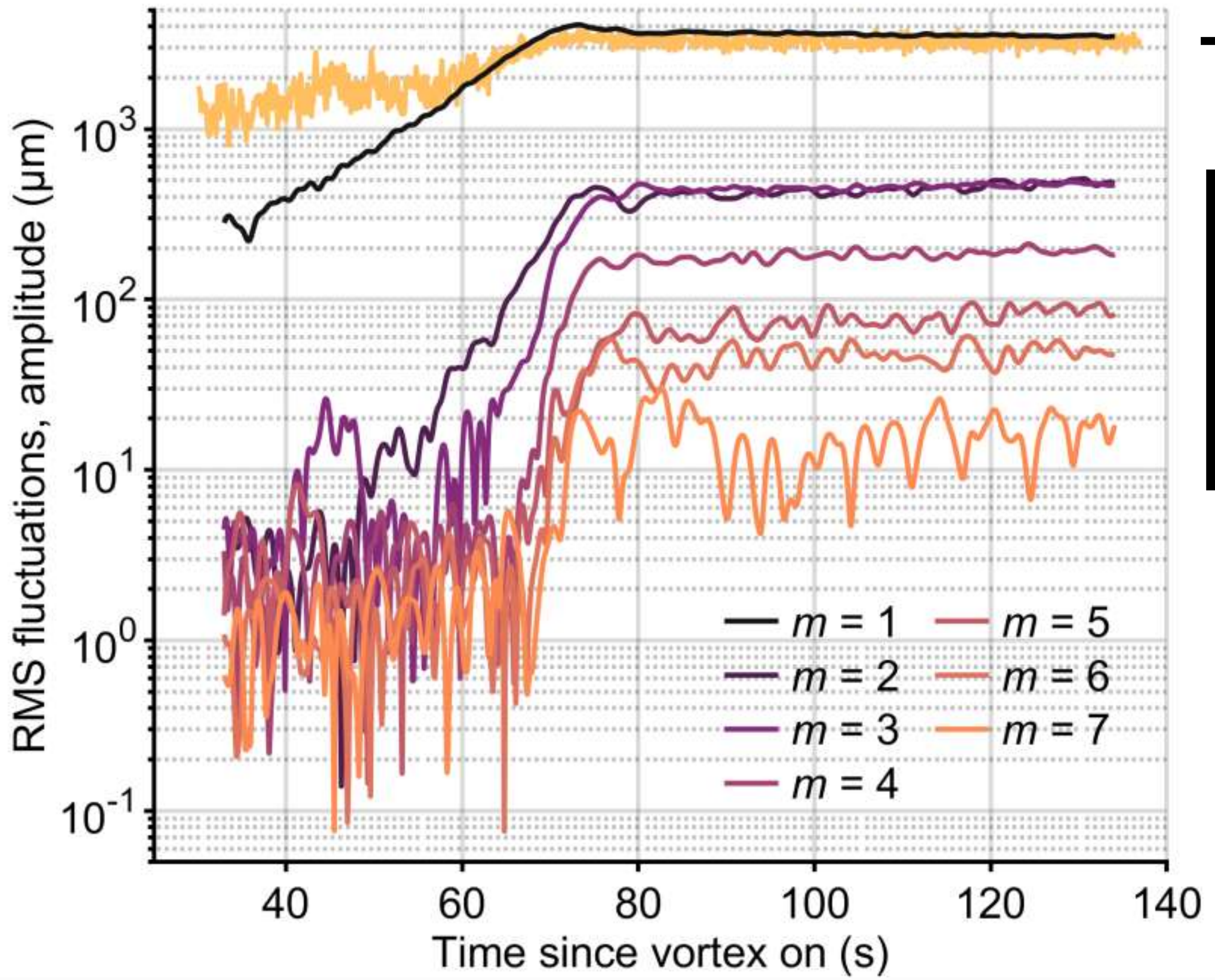

Primary mode: $m = 1, \omega_0 = 3.5Hz$

Excitations from **non-linear** interactions

$m = 2, \omega_2 = 2\omega_0$

$m = 3, \omega_3 = 3\omega_0$

...

Frequency Correlation Functions

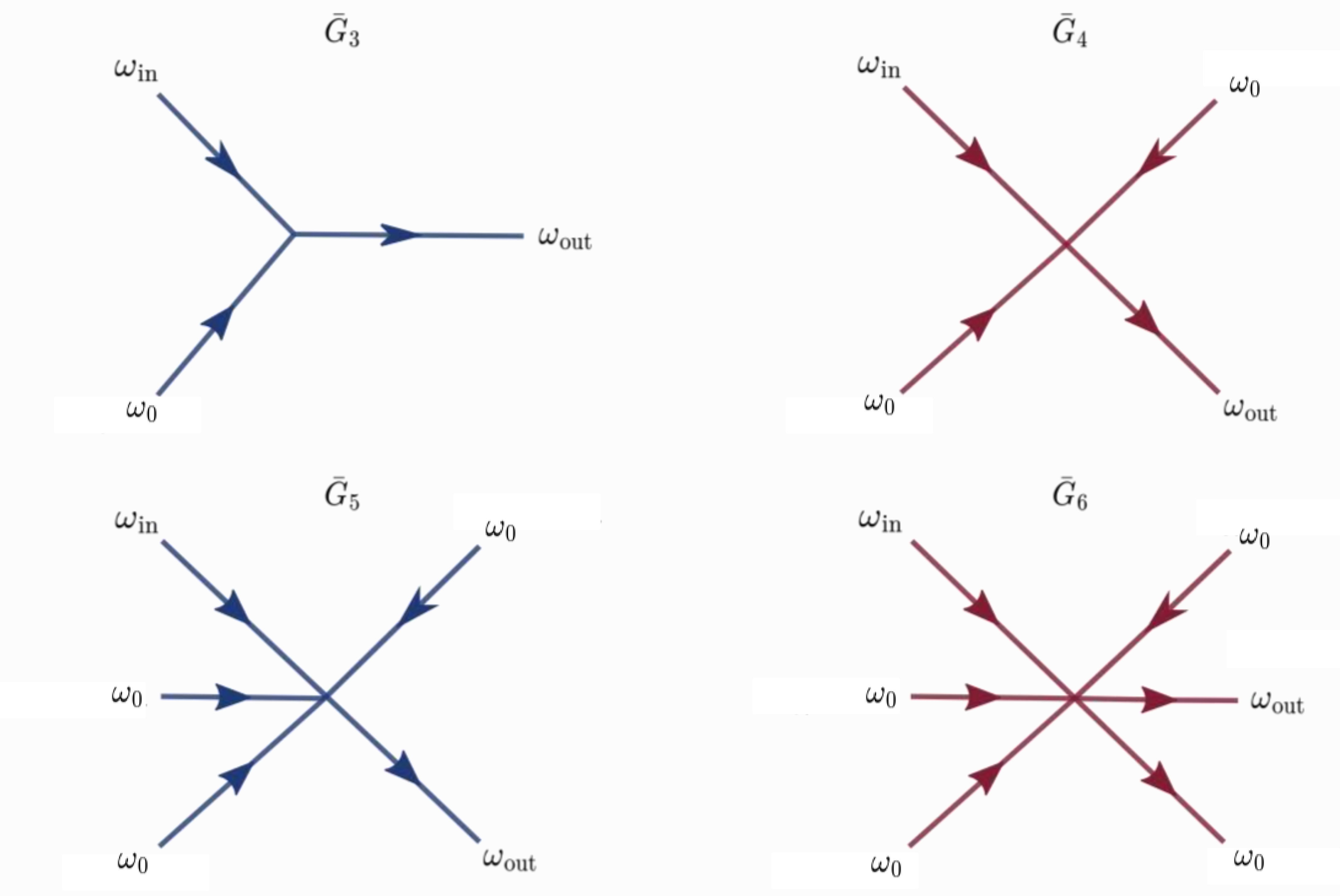

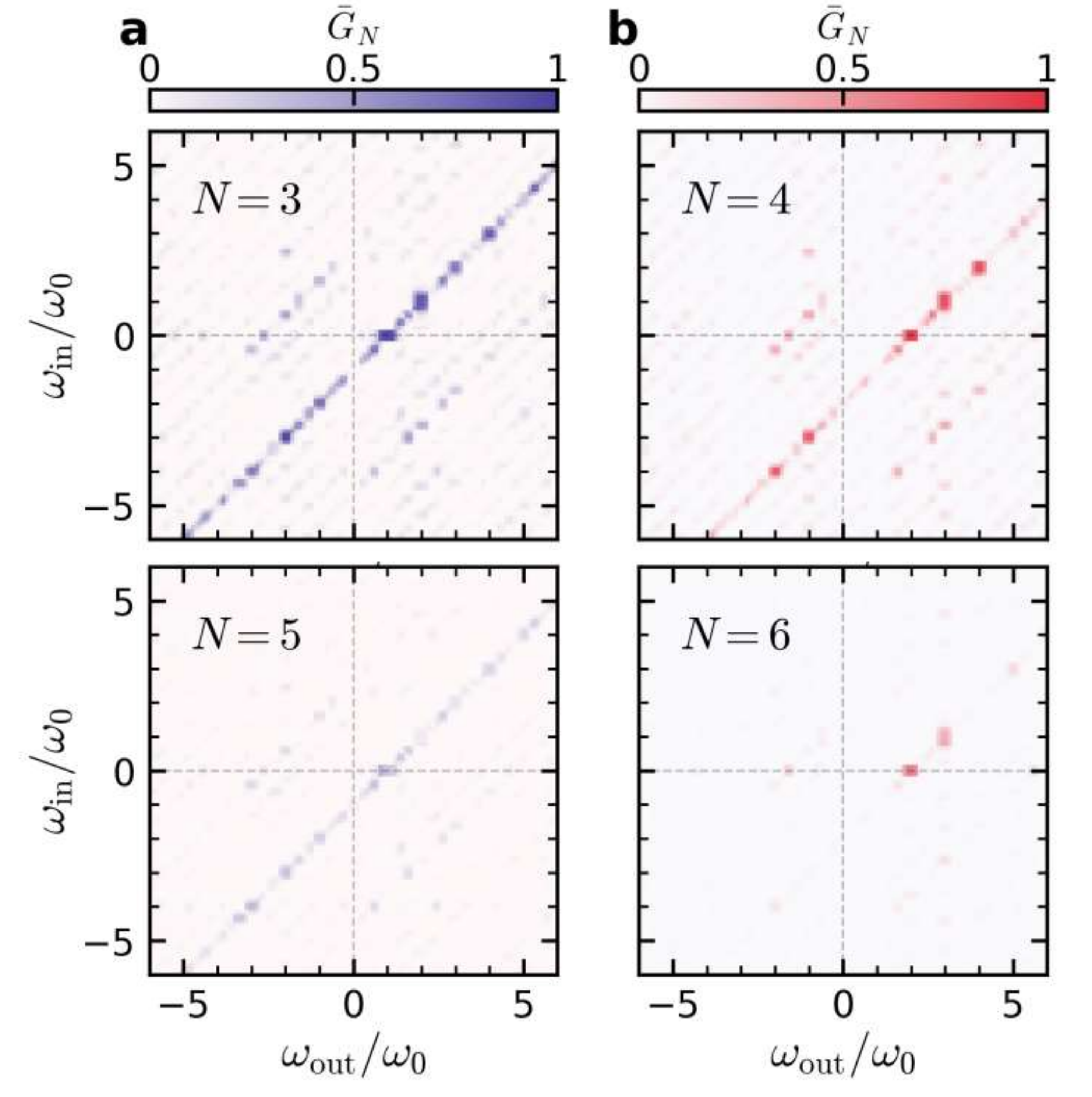

Conclusions

Fluid dynamical simulators of driven systems able to track nonlinear **interactions between waves** up to fully highly interactive stages

Observation of **conservation laws and hierarchy in the processes** moving energy
->"Shaker": Lagrangian description for a fully established out-of-equilibrium steady-state

Outlook

What can we learn from mutual information?

Application of similar techniques to other analogue simulators

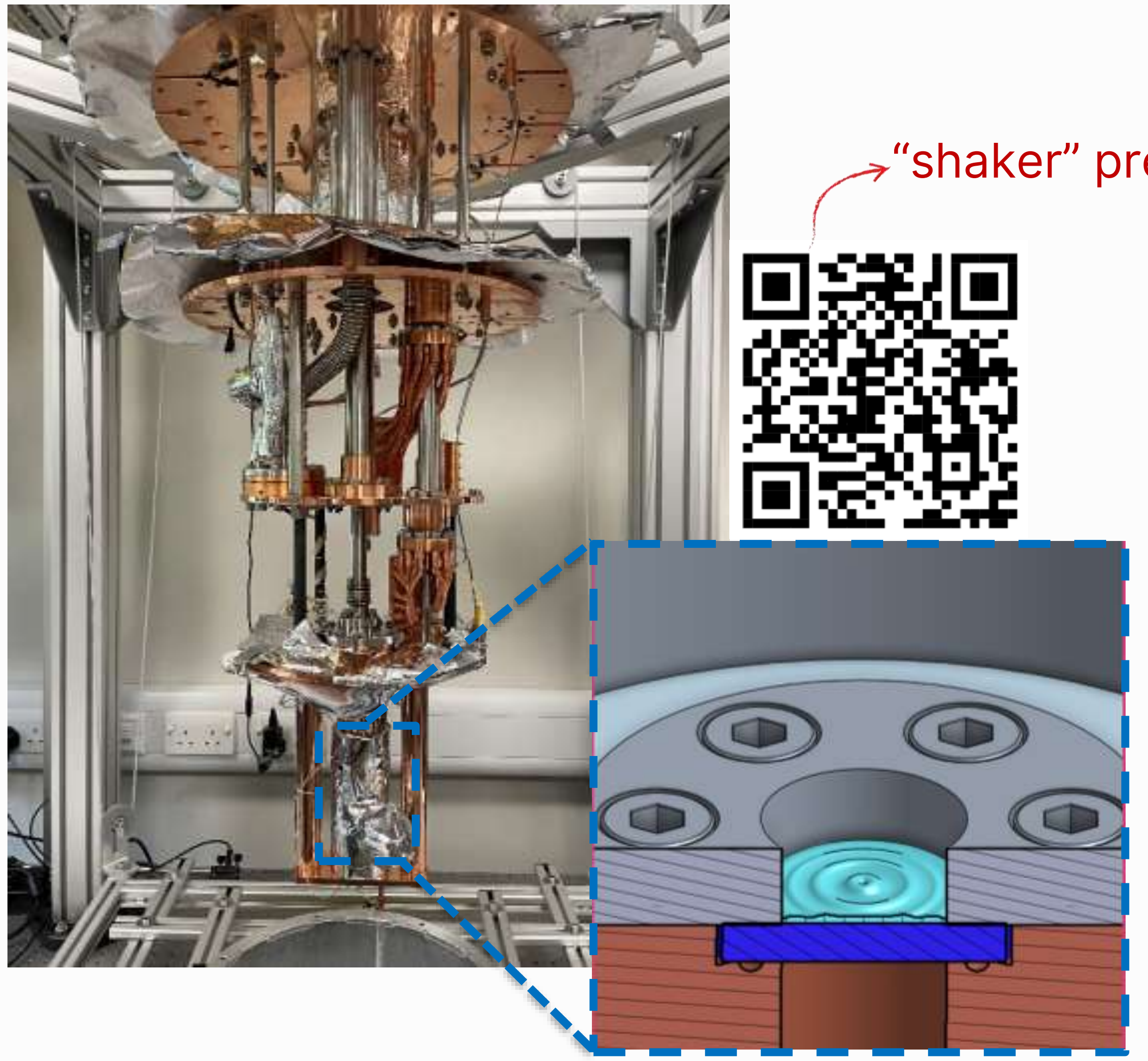

"shaker" preprint!

Conclusions

Fluid dynamical simulators of driven systems able to track nonlinear **interactions between waves** up to fully highly interactive stages

Observation of **conservation laws and hierarchy in the processes** moving energy
->“Shaker”: Lagrangian description for a fully established out-of-equilibrium steady-state

Outlook

What can we learn from mutual information?

Application of similar techniques to other analogue simulators

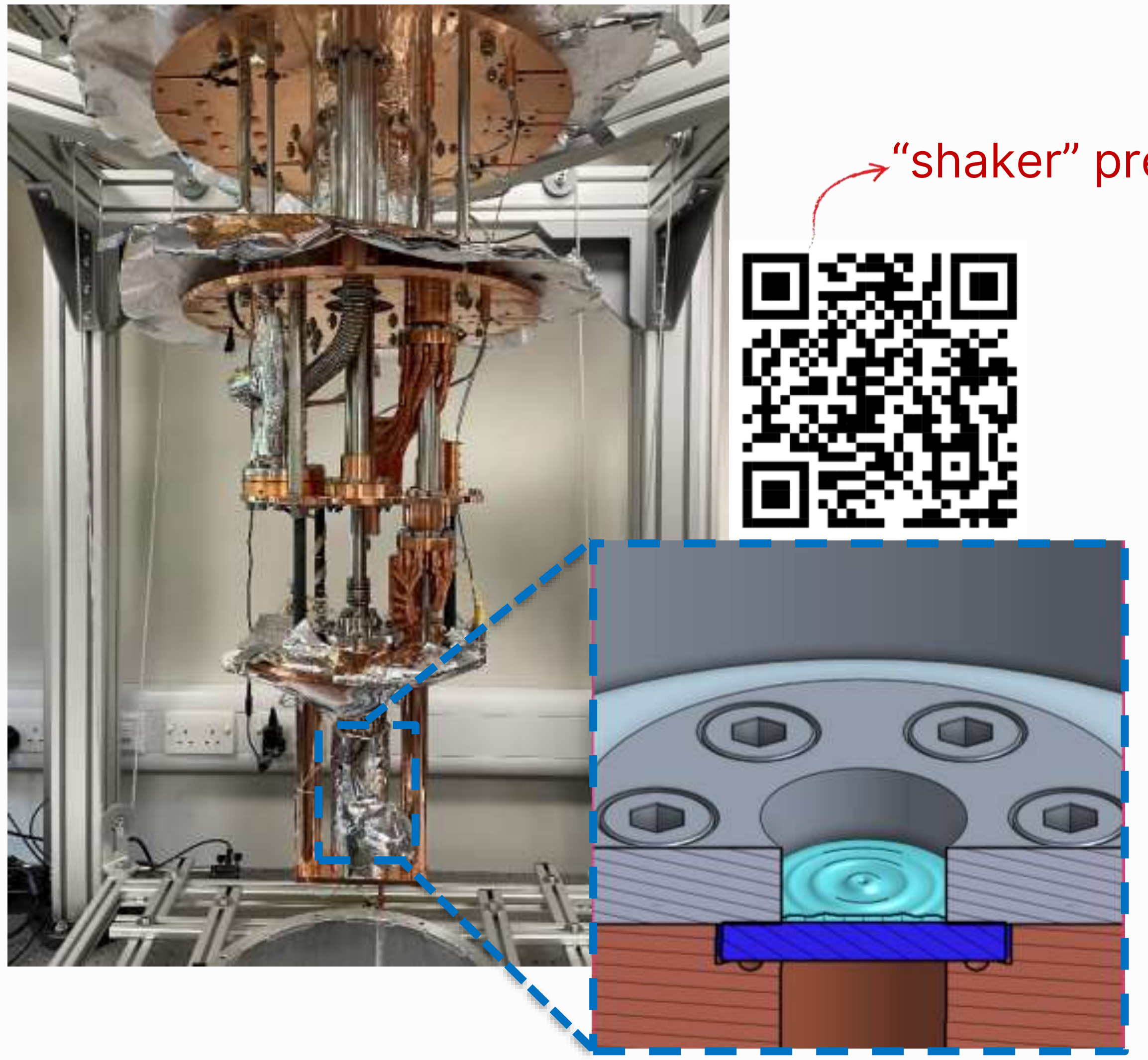

“shaker” preprint!

Questions?

silvia.schiattarella@nottingham.ac.uk

GRAVITY
LABORATORY

Analogue Simulators

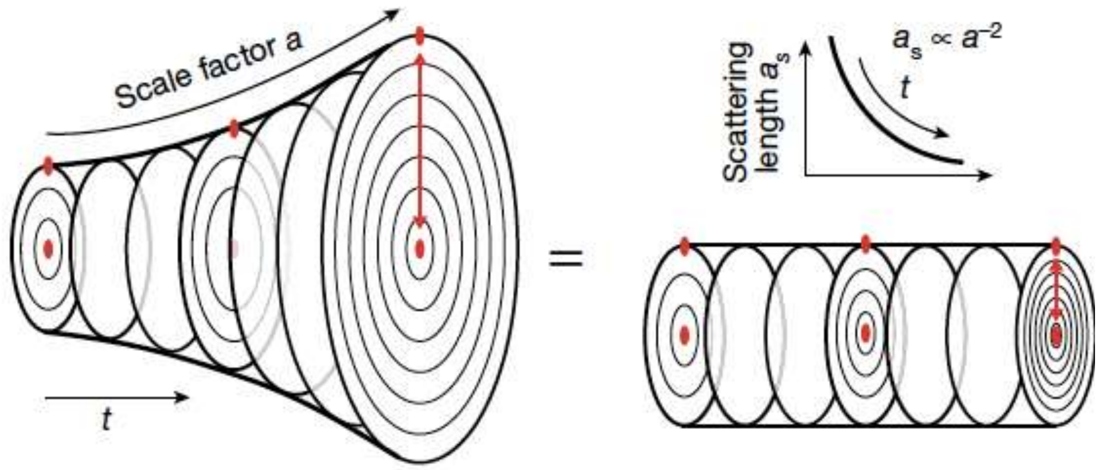

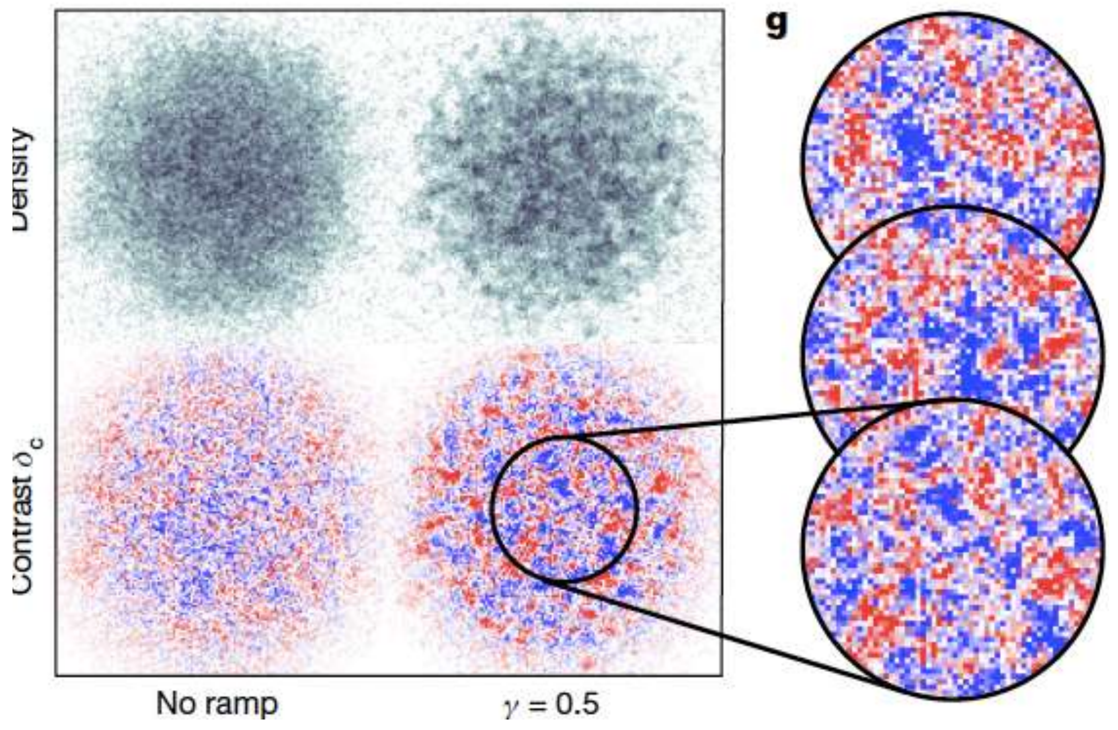

Particle creation

- Jaskula, J. C. *et al*, *Acoustic Analog to the Dynamical Casimir Effect in a Bose-Einstein Condensate*, *PRL*, **123**, 180502 (2012)
- Hung, C.L. *et al*, *From cosmology to cold atoms: observation of Shakarov oscillations in a quenched atomic superfluid*, *Science*, **341**, 1213-5 (2013)
- Steinhauer, J. *et al*, *Analogue cosmological particle creation in an ultracold quantum fluid of light*, *Nat. Comm.*, **13**, 2890 (2022)

Expanding geometries

- Eckel, S. *et al*, *A rapidly expanding Bose-Einstein condensate: An expanding Universe in the Lab*, *PRX*, **8**, 021021 (2018)
- Viermann, C. et al, *Quantum field simulator for dynamics in curved spacetime*, Nature, **611**, 260–264 (2022)

Cosmological reheating

- Chatrchyan, A. *et al*, *Analog cosmological reheating in an ultracold Bose gas*, *PRA*, **104**, 023302 (2021)
- Gregory, S., Schiattarella S. *et al*, *Tracking the nonlinear formation of an interfacial wave spectral cascade from one to few to many*, **arXiv:2410.08842**

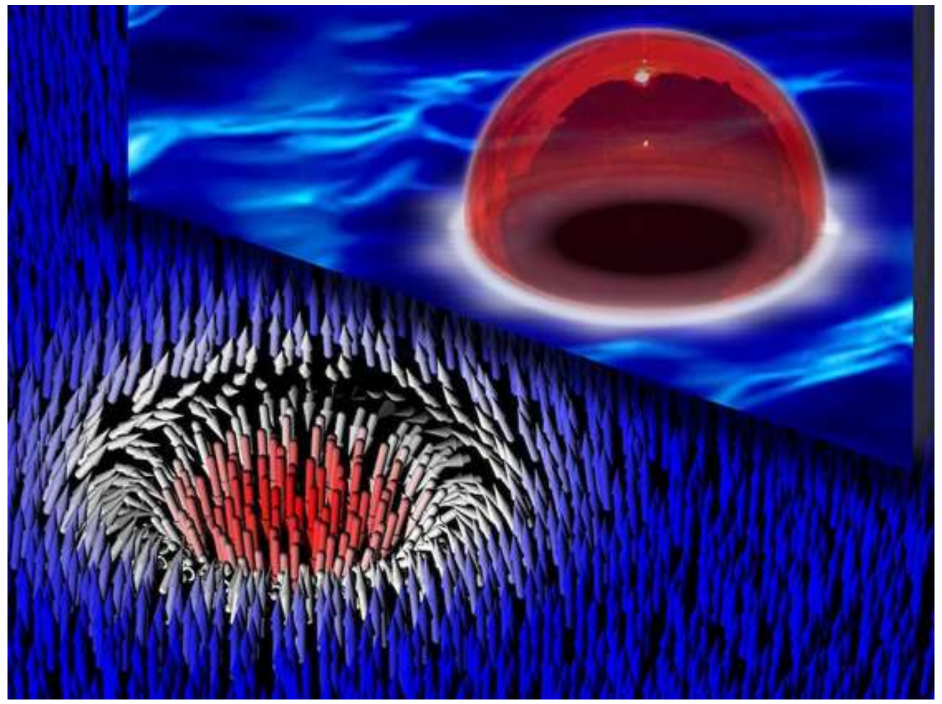

False Vacuum Decay

- Jenkins, A. C. *et al*, *Generalized cold-atom simulators for vacuum decay*, *PRA*, **110**, L031301 (2022)
- Zanesini, A. *et al*, *False vacuum decay via bubble formation in ferromagnetic superfluids*, *Nat. Phys.*, **20**, 558–563 (2024)
- Jenkins, A. C. *et al*, *Analog vacuum decay from vacuum initial conditions*, *PRD*, **109**, 023506 (2024)

Analogue Simulators

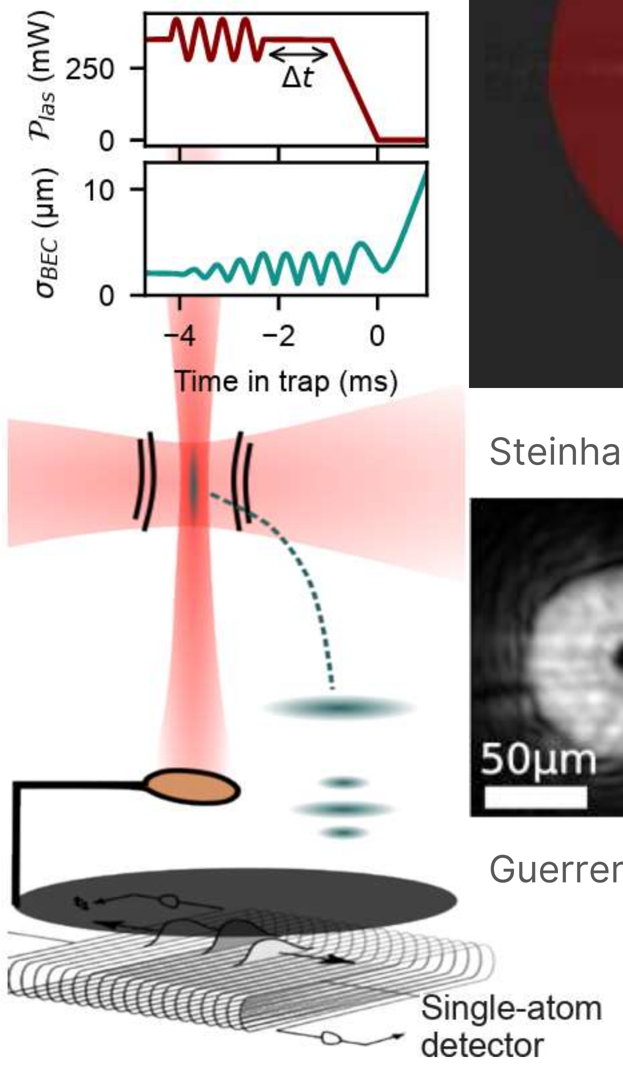

Gondret, V. *et al*, *PRL*, **135**, 240603 (2025)

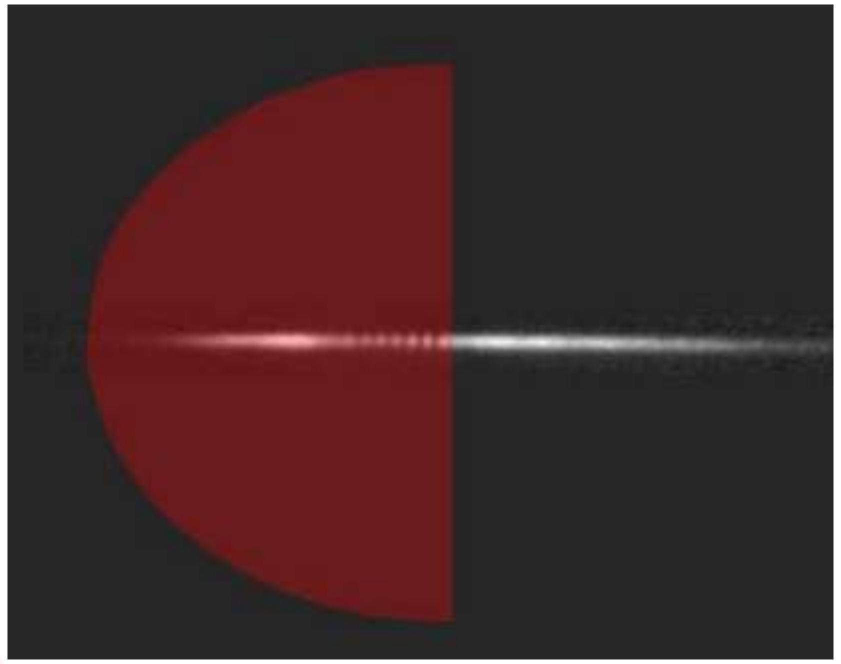

Steinhauer, J. ,*Nat. Phys.*, **12**, 959–965 (2016)

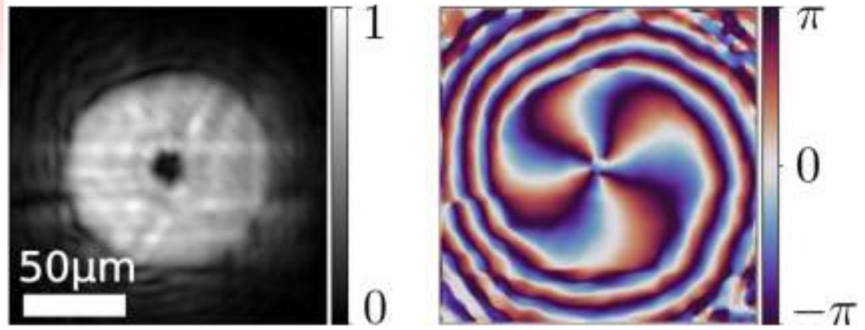

Guerrero, K. *et al*, *PRL*, **135**, 243801 (2025)

Viermann, C. et al, *Nature*, **611**, 260–264 (2022)

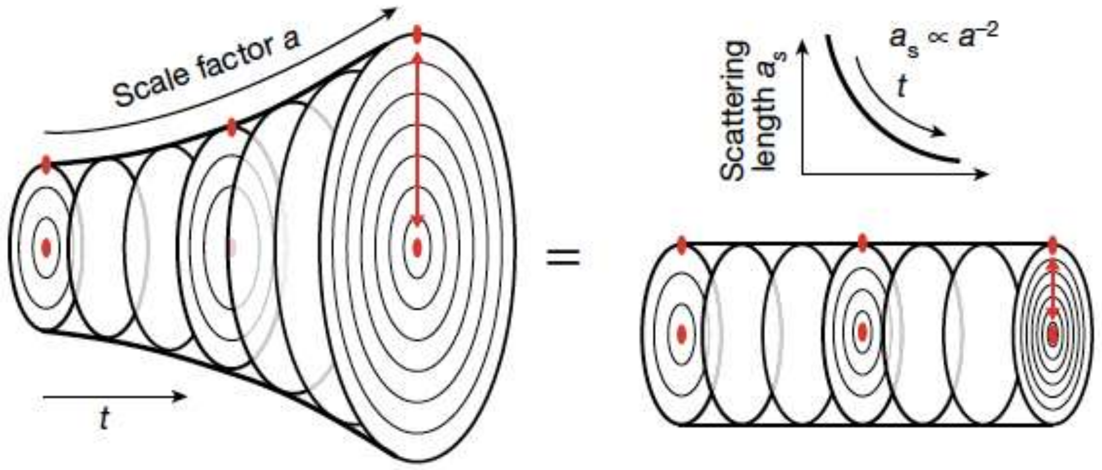

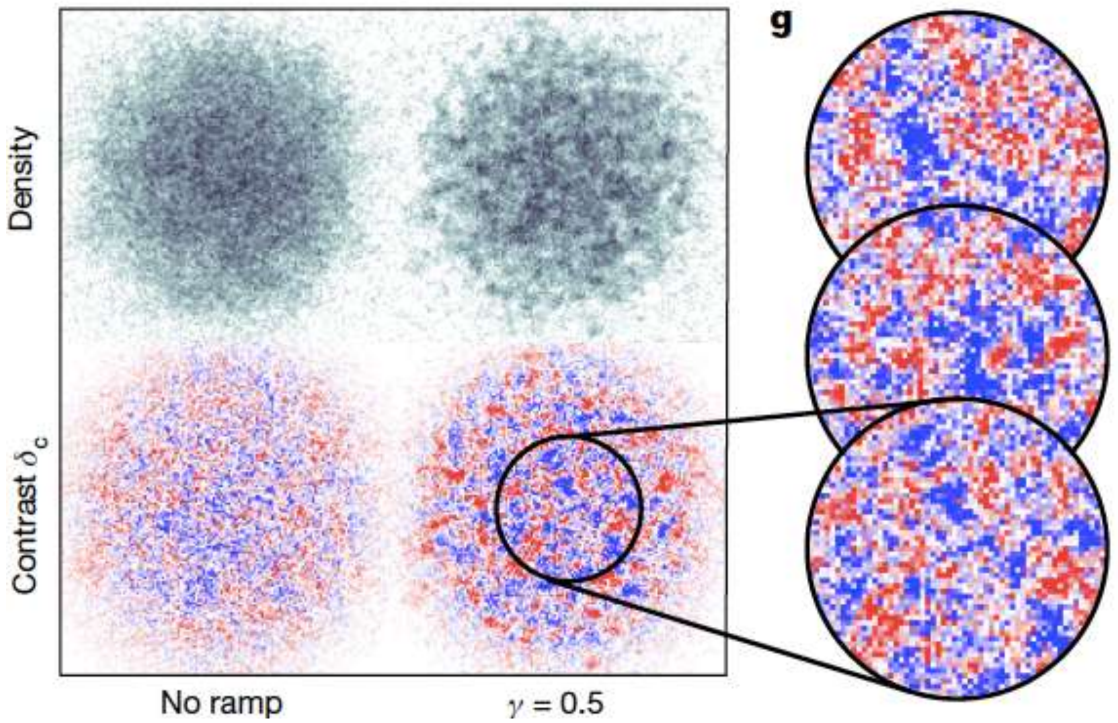

Zenesini, A. *et al*, *Nat. Phys.*, **20**, 558–563 (2024)

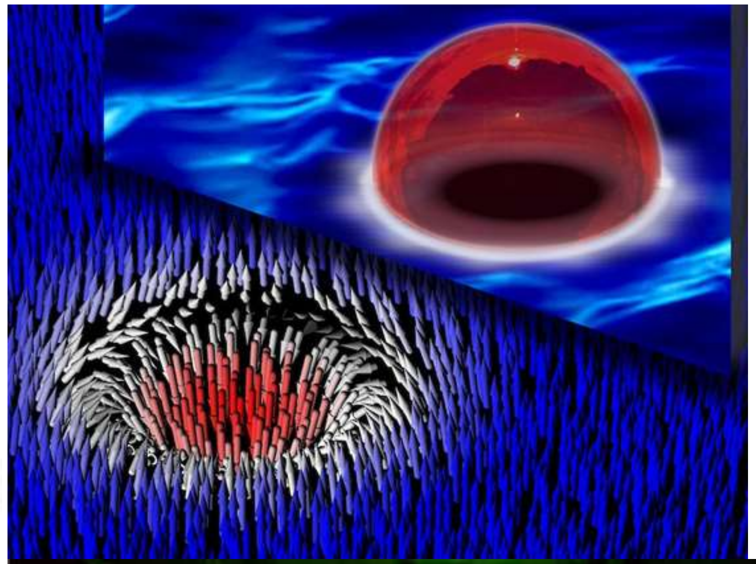

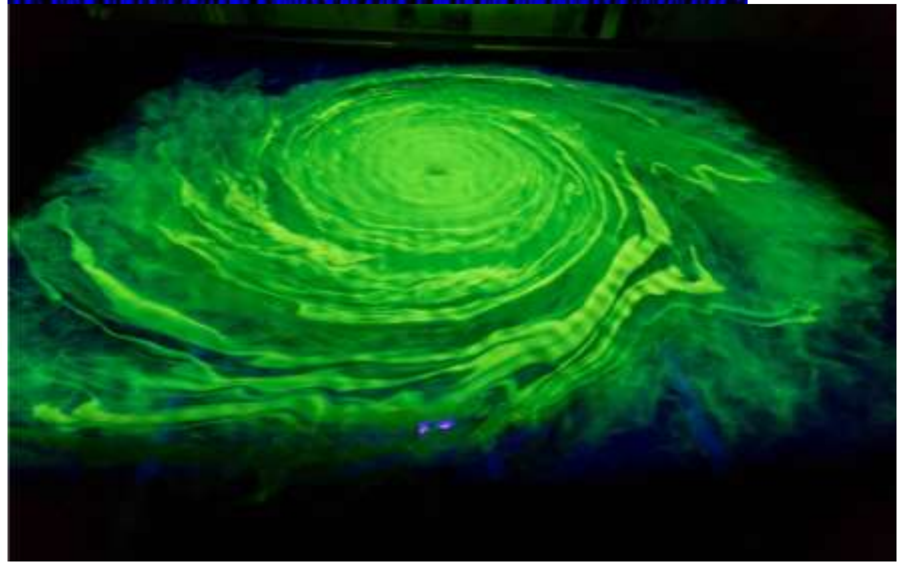

Torres, T. *et al*, *Nat. Phys.*, **13**, 833–836 (2017)

Parametric resonance in past studies

Bands of Resonance

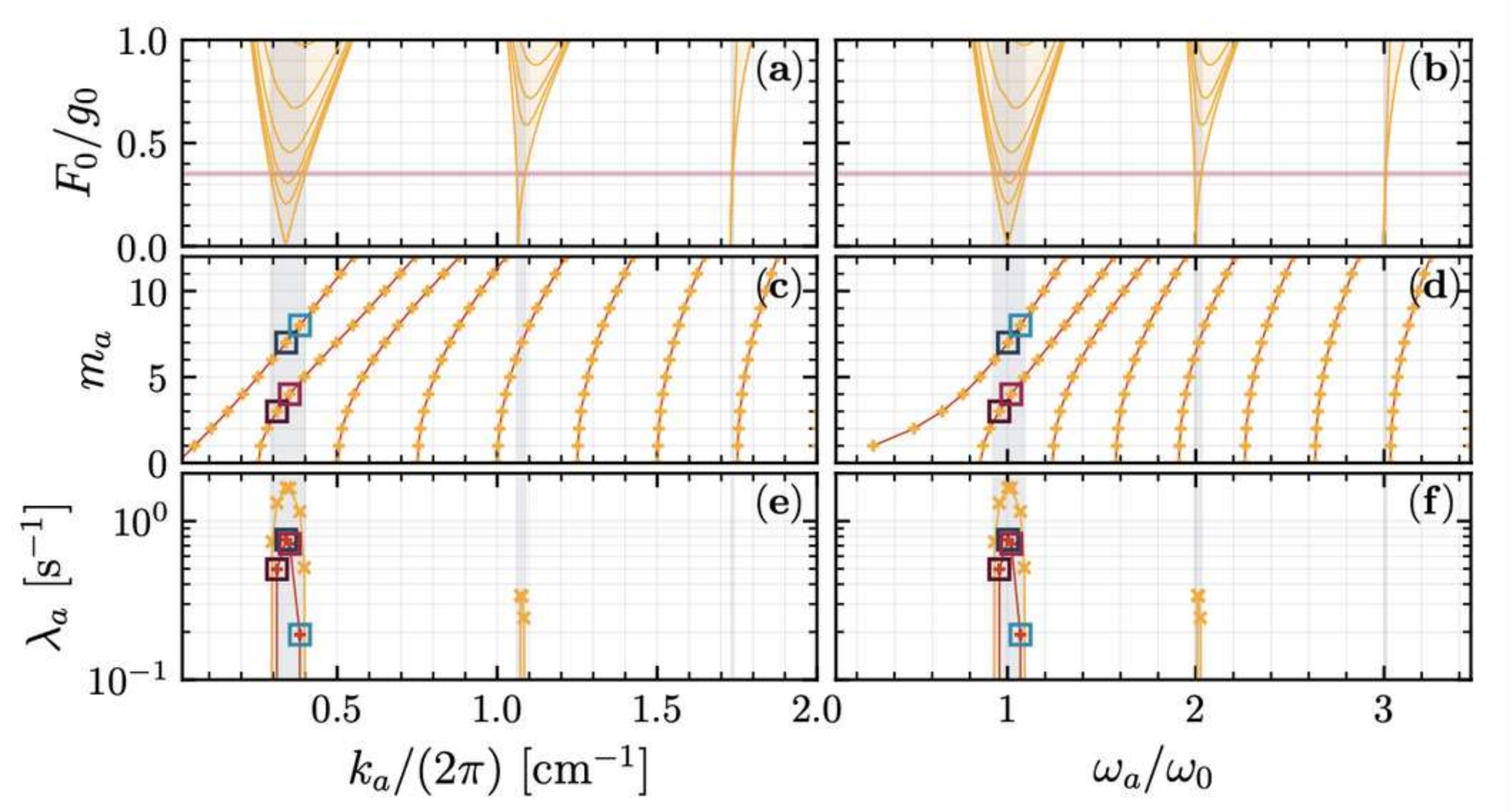

The mode m=4 will be excited with a certain value for the slope λ

Secondary Instabilities

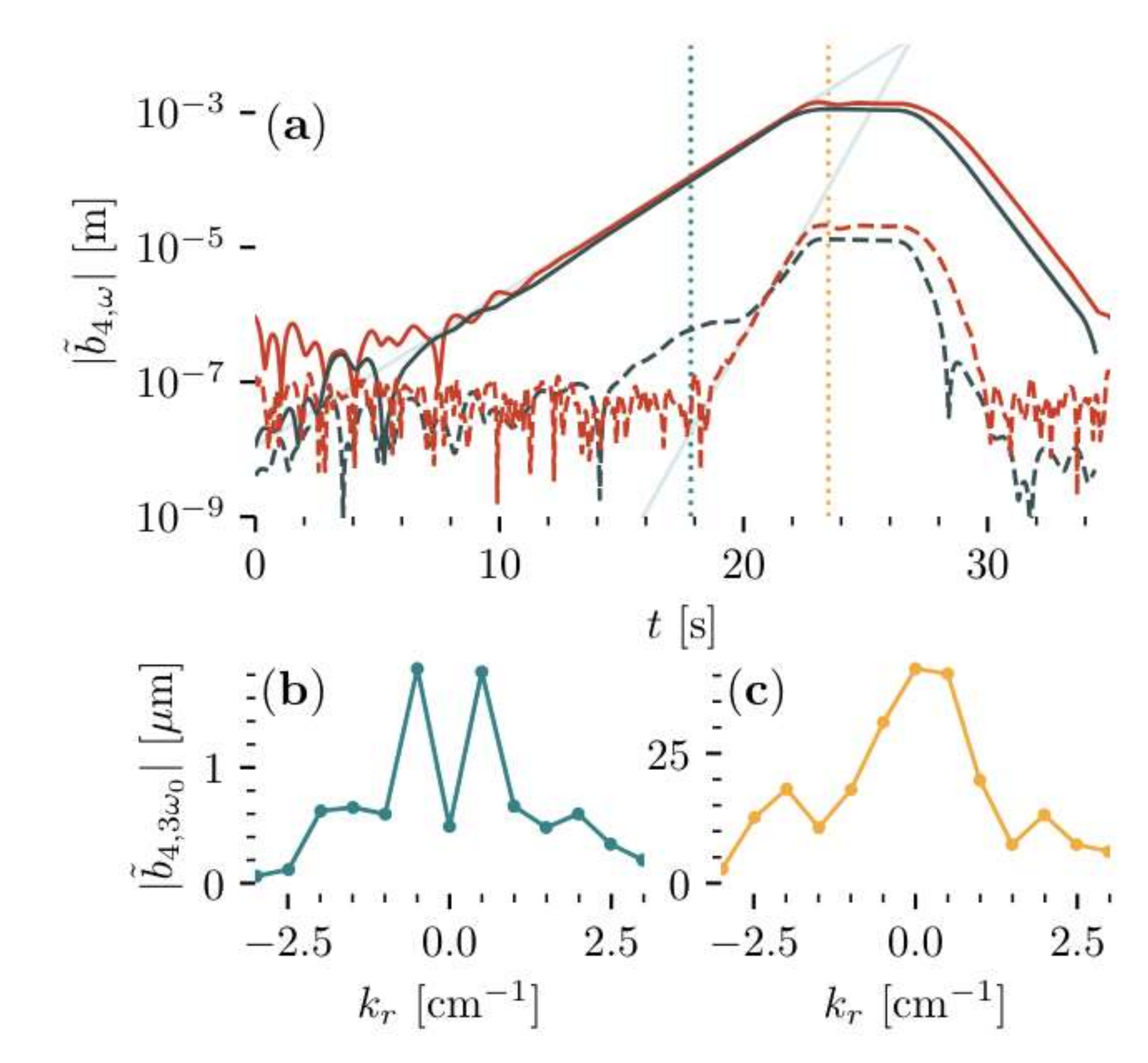

Parametric resonance

Theoretical model

Available excitations through parametric resonance

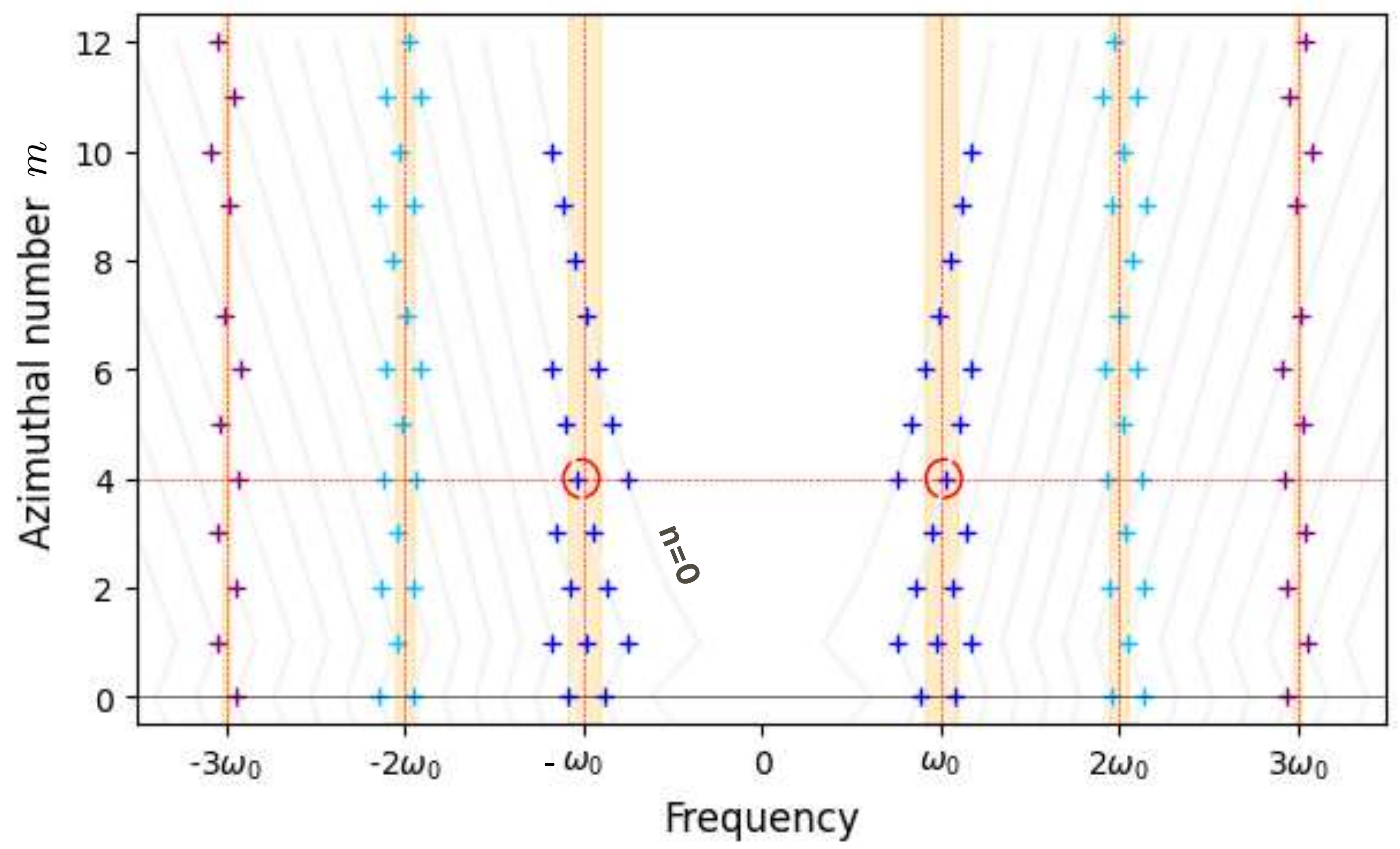

Experimental observation

$(4,1)_{\pm\omega_0}$ Dominant excitation

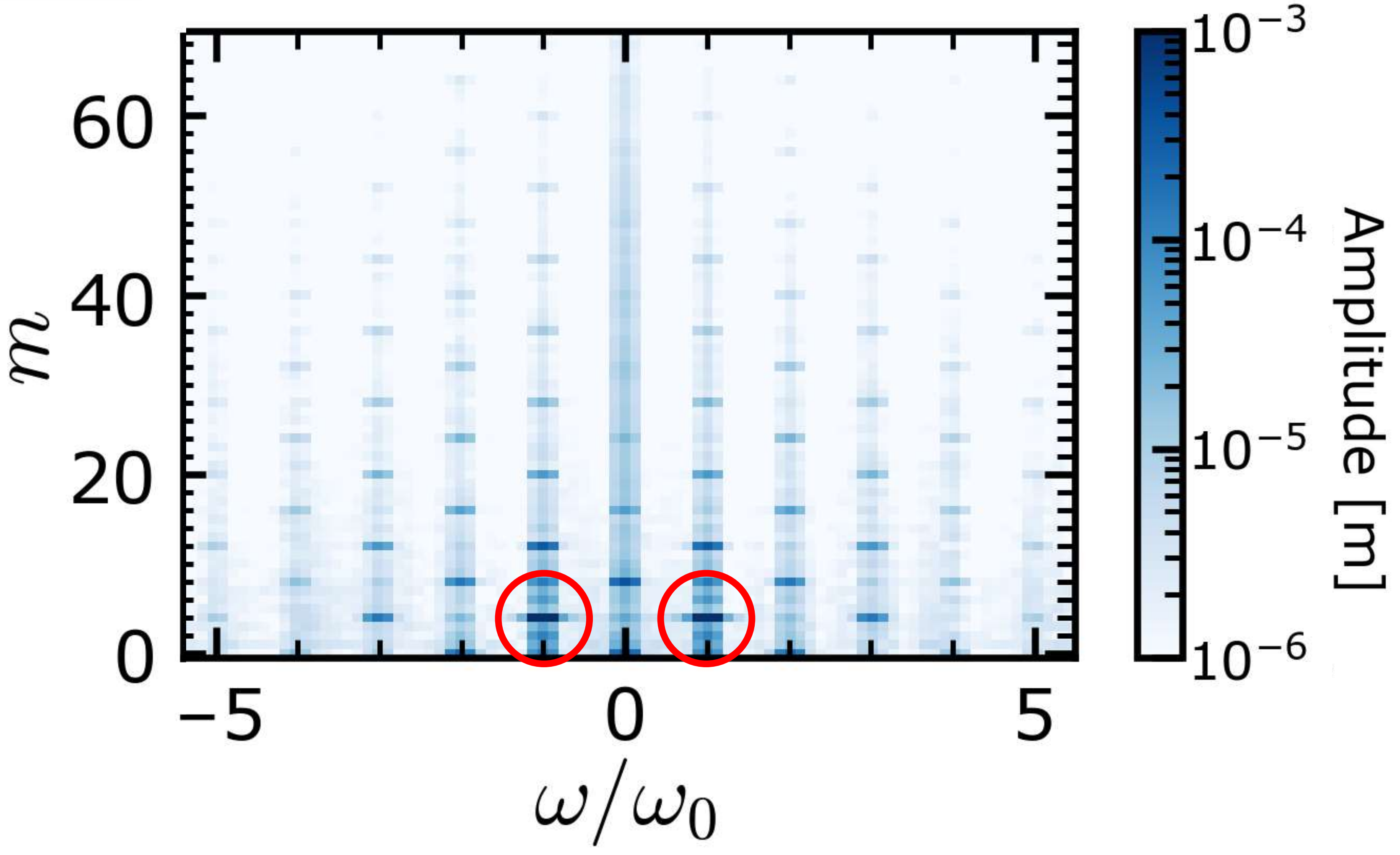

$$\xi_a(t) = \xi_a e^{i\omega t} + \xi_a e^{-i\omega t}$$

Correlation Functions

Time correlation functions

$$g_N(\xi_1 \dots \xi_N) = \langle \xi_1 \dots \xi_N \rangle$$

$$\xi_i \equiv \xi_{m,\omega}(t,r)$$

g_N averaged over experimental runs, r, θ:

$$\bar{g}_N(t) \equiv \frac{|\langle \xi_1 \dots \xi_N \rangle_c|}{\langle |\xi_1 \dots \xi_N| \rangle}$$

Frequency correlation functions

$$G_N(\omega_1, \dots, \omega_N) = \langle \xi_{\omega_1} \dots \xi_{\omega_N} \rangle$$

$$G_N(\omega_1, \dots, \omega_N) = \sum_{m_1, \dots, m_N} g_N(\xi_{m_1,\omega_1} \dots \xi_{m_N,\omega_N})$$

G_N averaged over experimental runs, t, r, θ:

$$\bar{G}_N(\omega_1, \dots, \omega_N) = \frac{|\langle \xi_{\omega_1} \dots \xi_{\omega_N} \rangle_c|}{\langle |\xi_{\omega_1} \dots \xi_{\omega_N}| \rangle}$$

Correlation Functions

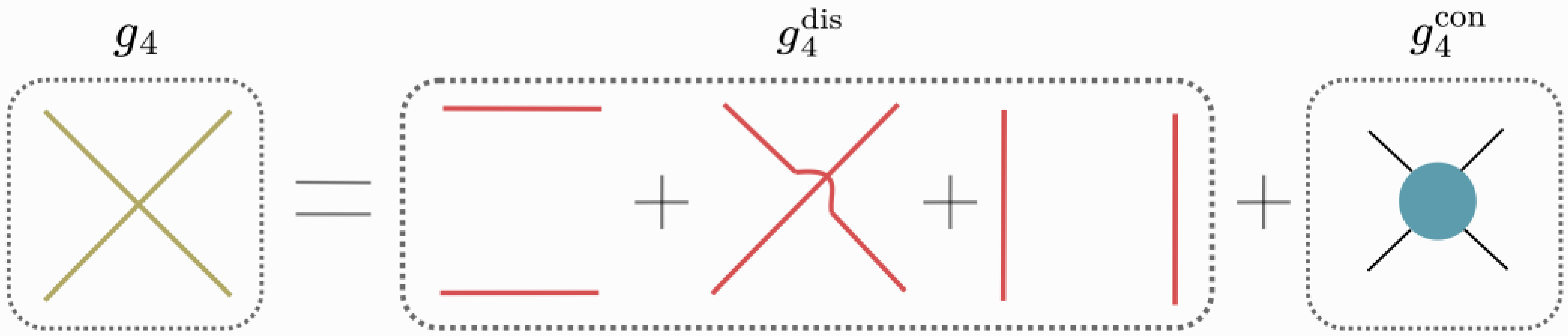

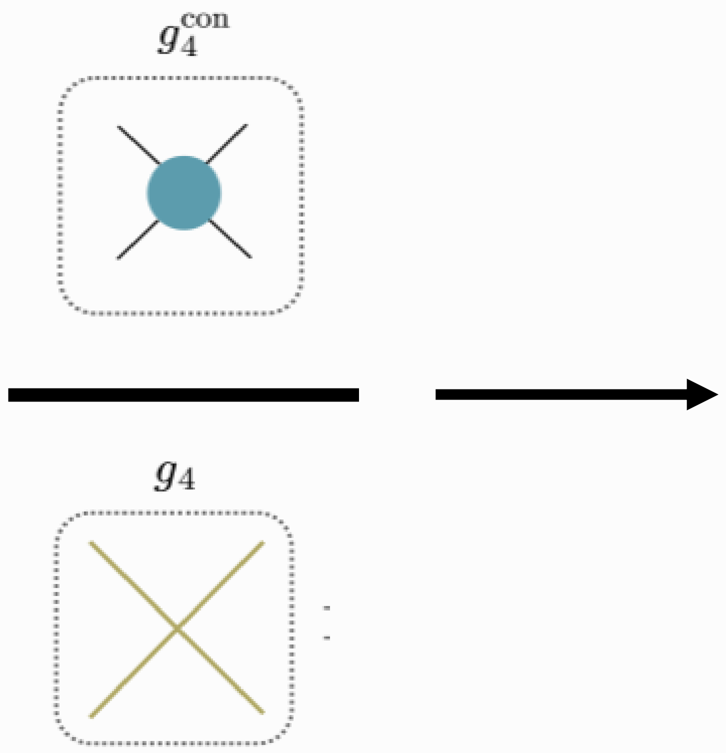

$$\begin{cases} \bar{g}_N(t) \equiv \dfrac{|\langle \xi_1 \dots \xi_N \rangle_c|}{\langle |\xi_1 \dots \xi_N| \rangle} \\ \bar{G}_N(\omega_1, \dots, \omega_N) = \dfrac{|\langle \xi_{\omega_1} \dots \xi_{\omega_N} \rangle_c|}{\langle |\xi_{\omega_1} \dots \xi_{\omega_N}| \rangle} \end{cases}$$

Secondary instabilities

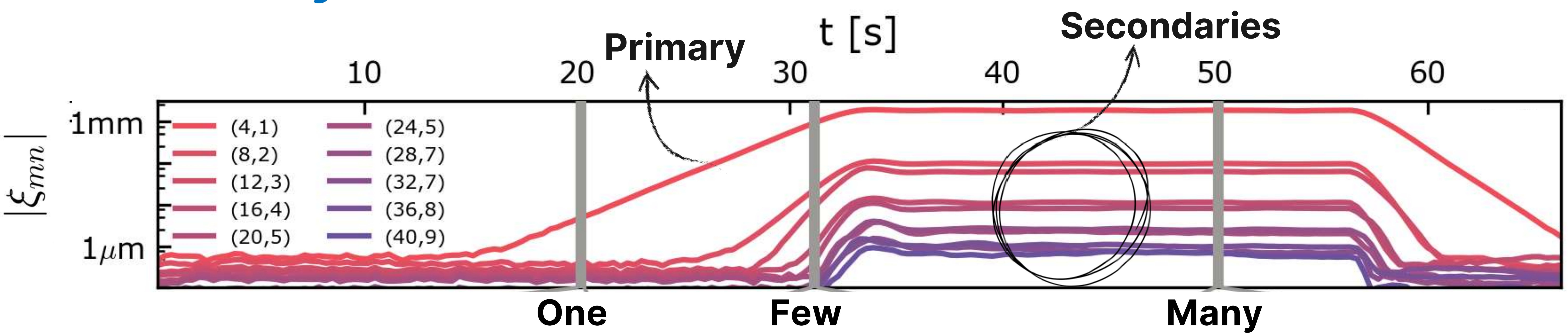

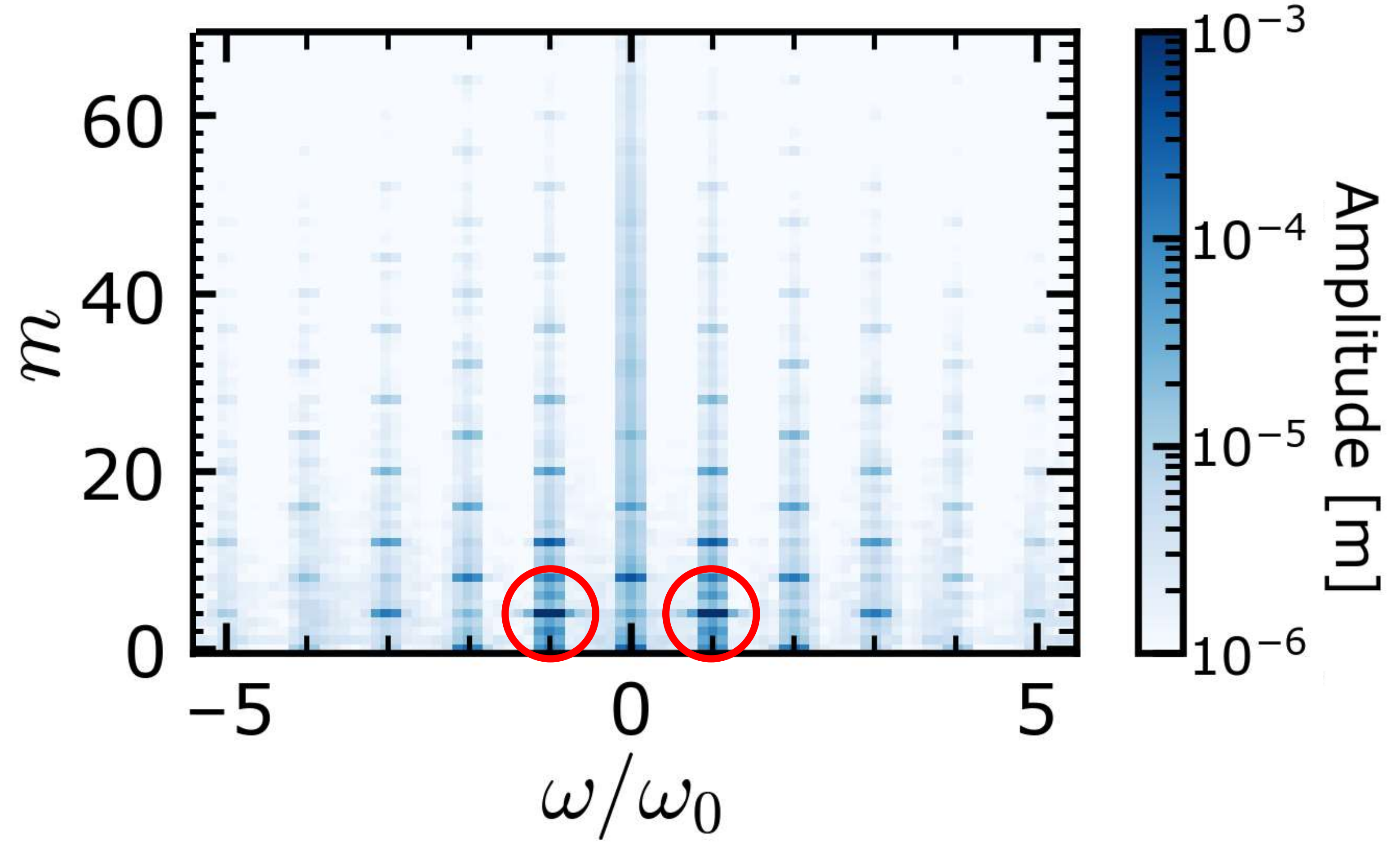

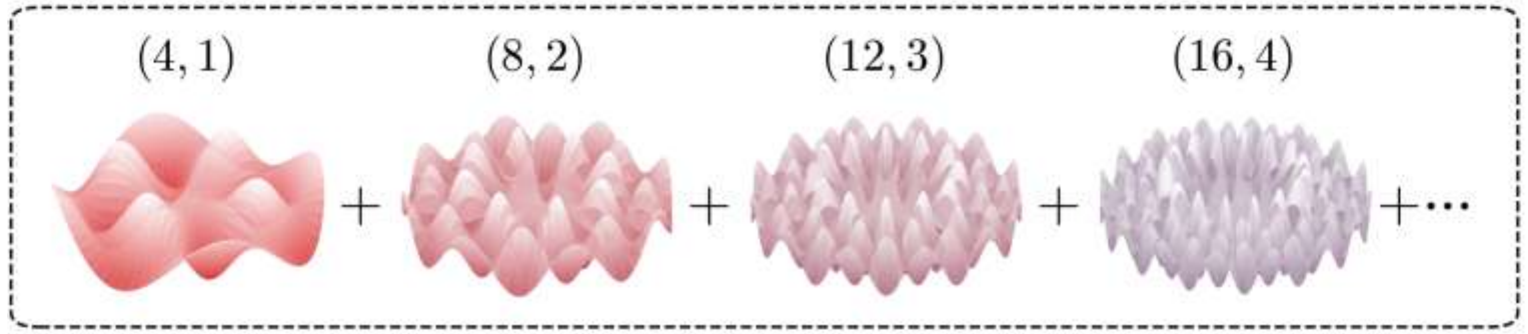

From *few* to *many*

FEW REGIME: ***t = 25 s***   ***MANY*** REGIME: ***t = 40 s***

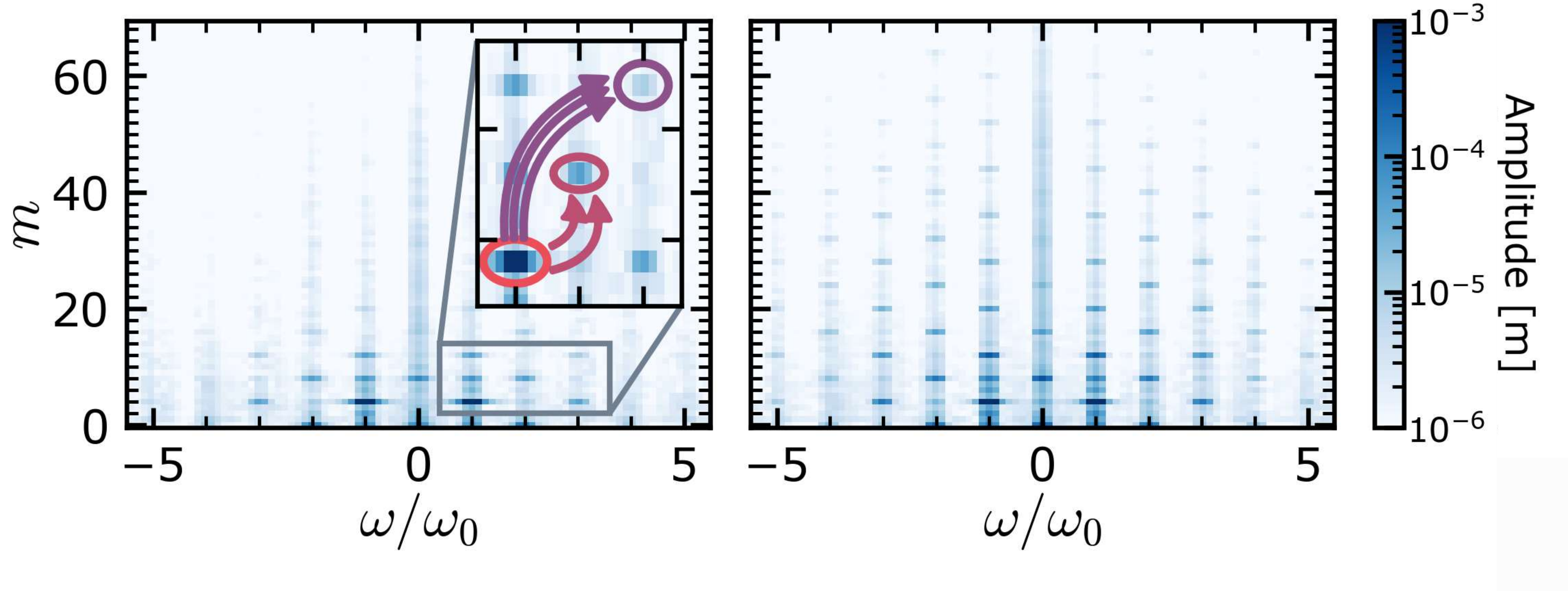

Many interacting waves

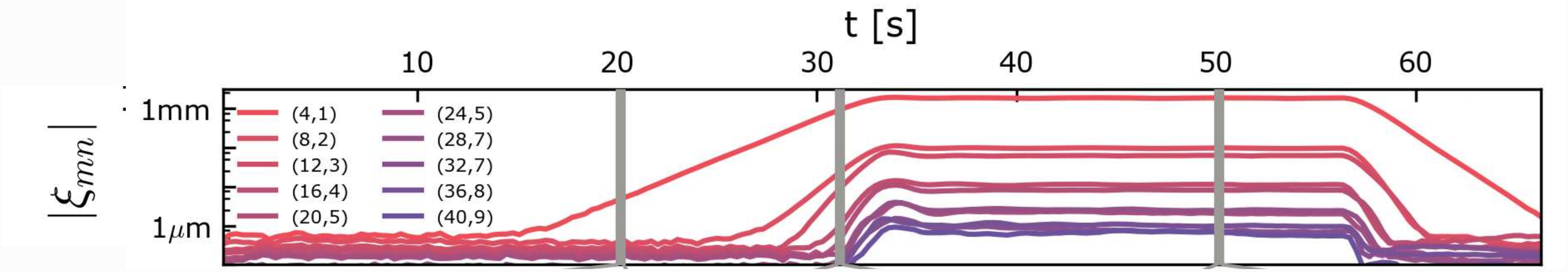

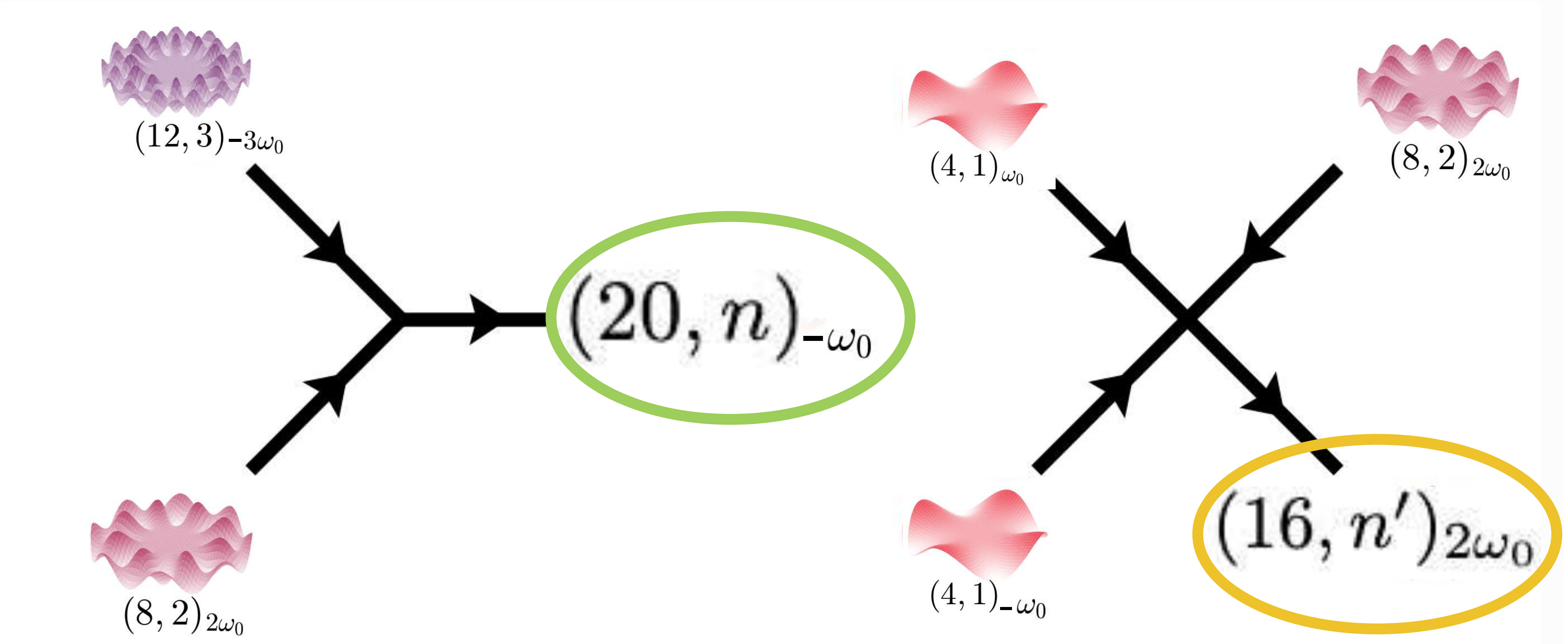

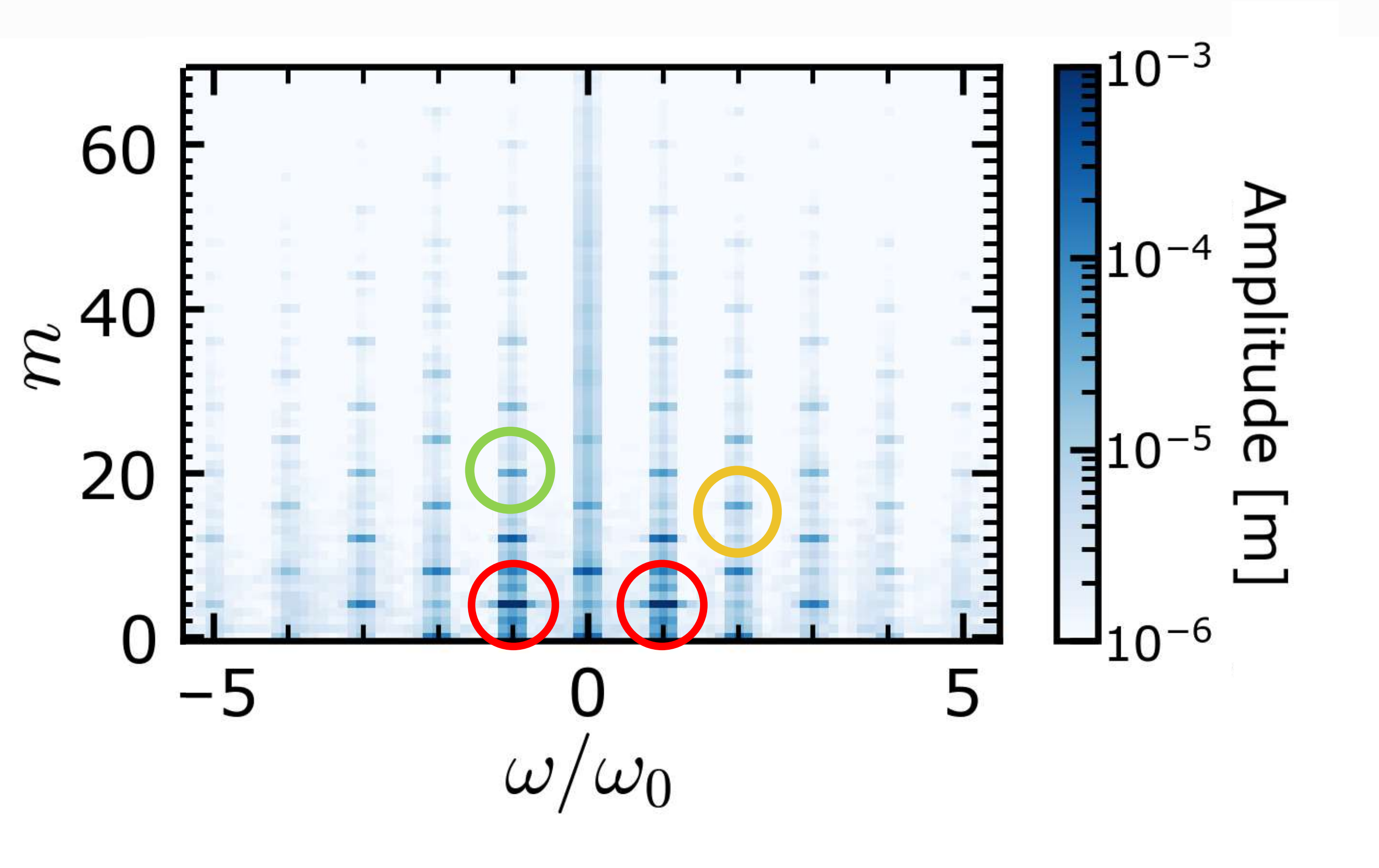

Two dominant modes

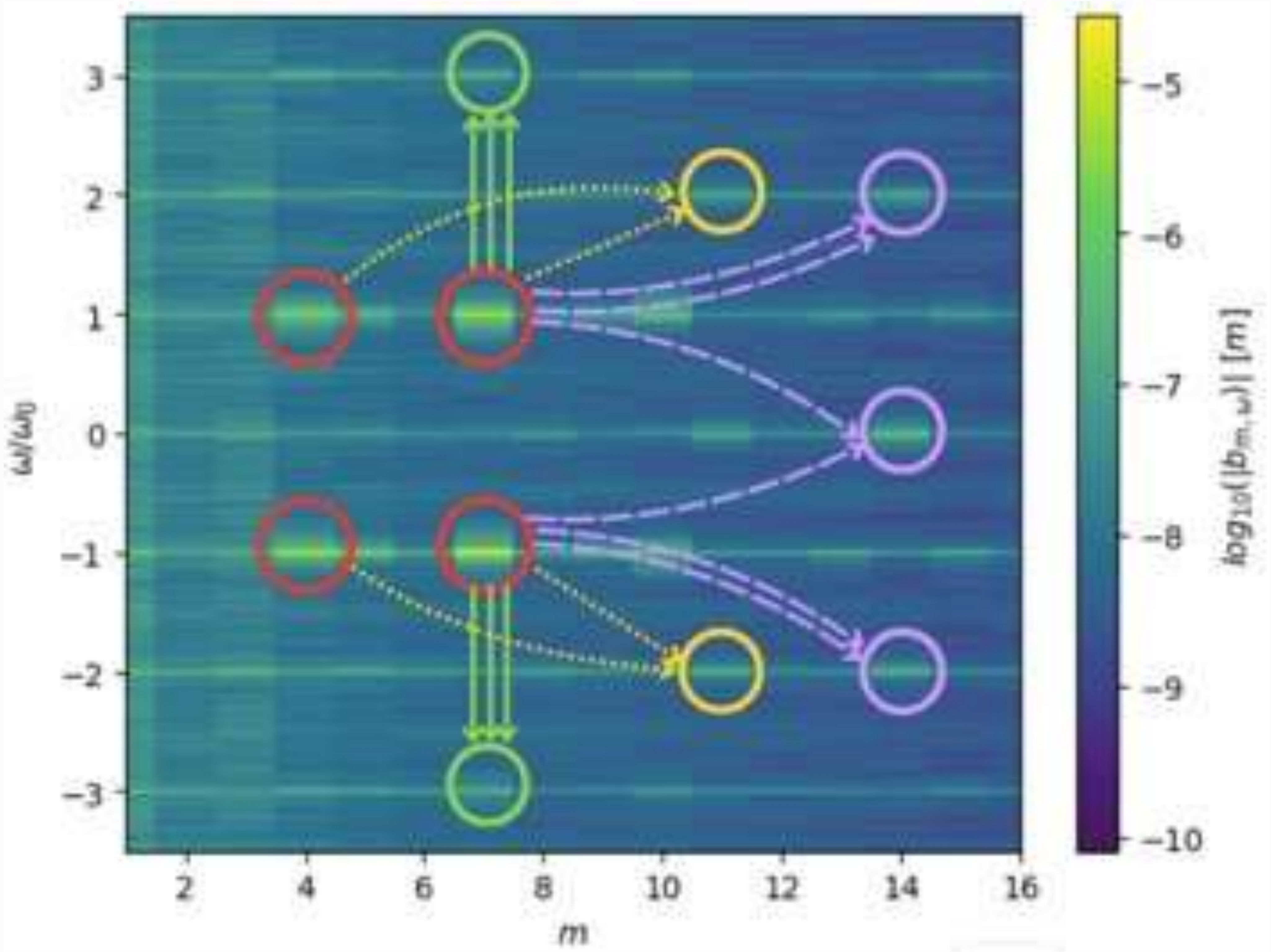

Growth-decay analysis

Cubic and quartic interactions

$\xi_a \propto \exp(\lambda_a t + i n \omega_0 t)$

SLOPES

DAMPING

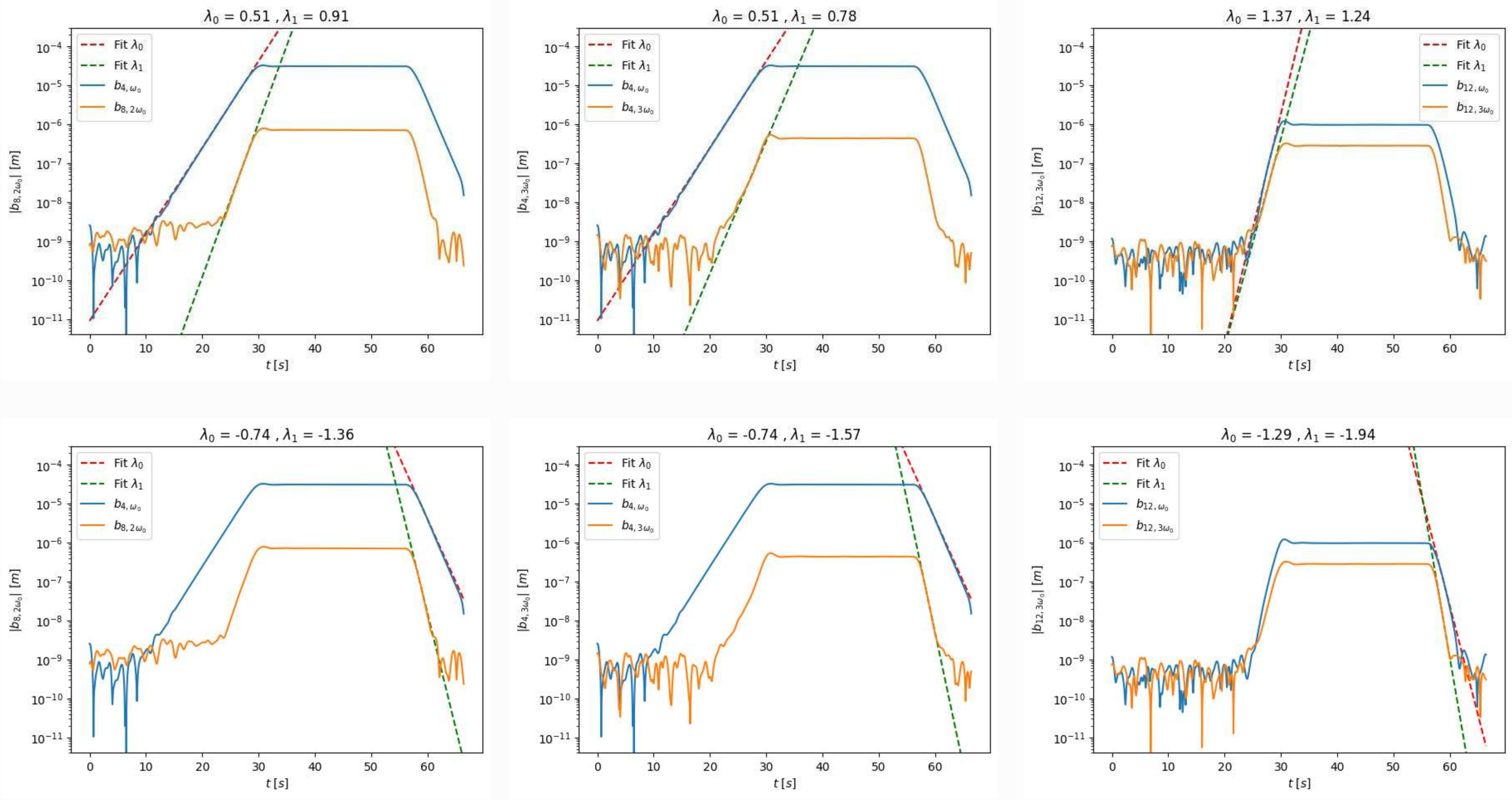

Dynamics

Equation of motion:

$$\ddot{\xi}_a + 2\gamma_a\dot{\xi}_a + \omega_a^2\xi_a = 0$$

$$\frac{d}{dt}\left(\frac{\partial L}{\partial \dot{\xi}_a}\right) - \frac{\partial L}{\partial \xi_a} = -\frac{\partial Q_0}{\partial \dot{\xi}_a}$$

Floquet solutions:

$$\xi_a = \sum_n \zeta_{a,n} \exp(\lambda_a t + in\frac{\omega_d}{2}t), \text{ with } \lambda_a > 0$$

Drive-dependent frequency:

$$\ddot{\xi}_{km} + 2\gamma_k\dot{\xi}_{km} + (\omega_k^2 - \Omega_k^2(t))\xi_{km} = \eta_k(t)$$

$$F(t) = F_0\cos(2\omega_0 t)$$

$$\omega_a^2 = \frac{(\rho_1 - \rho_2)g(t) + \sigma k_a^2}{\rho_1 + \rho_2} k_a \tanh(k_a h_0)$$

$$\Omega_k^2(t) = F(t)\frac{\rho_1 - \rho_2}{\rho_1 + \rho_2} k\tanh(kh_0)$$

Set up

•Immiscible two-fluid system
•Two sets of coupled Navier-Stokes equations
•Explicitly time-dependent system
•Confinement (velocities vanish at cell boundaries)
•
•Acceleration platform (repeatable driving)
•spring-mass system was driven by a voice-coil actuator
•pneumatic bearings (frictionless air surface air~10μm)
•Mounted on noise-isolation platform
•Computer operated
•
•Monitoring
•High-precision accelerometers
•Temperatures sensors were at strategic locations

•Detection method
•Adapted Fourier Transform Profilometry
•Continuous wavelet analysis (time-frequency analysis)

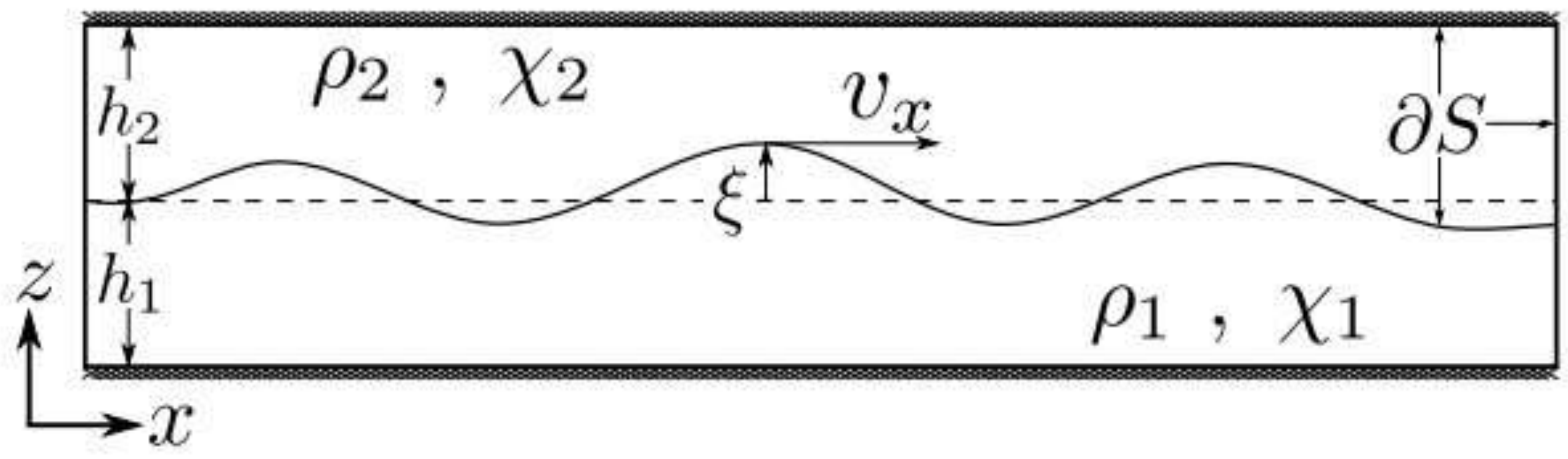

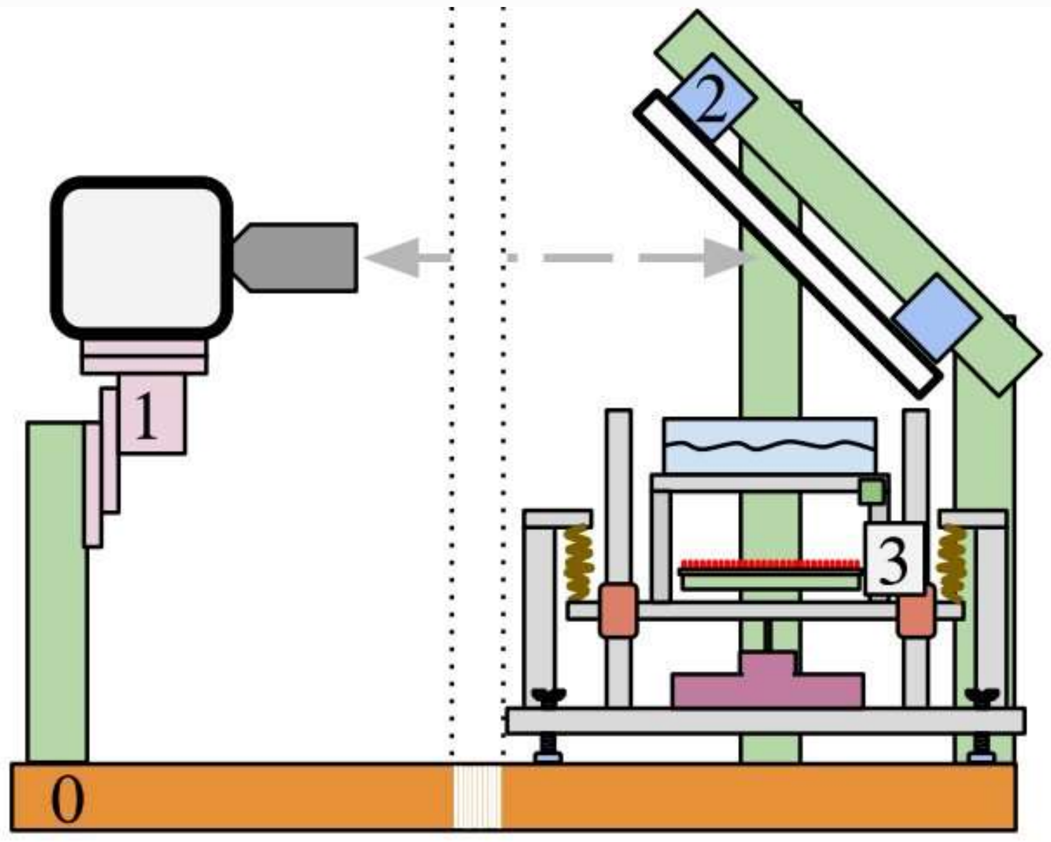

Correlations

Thermal field theory techniques to investigate wave-mixing:

•Higher-order equal-time full correlation functions

•Extract Disconnected equal-time correlation functions

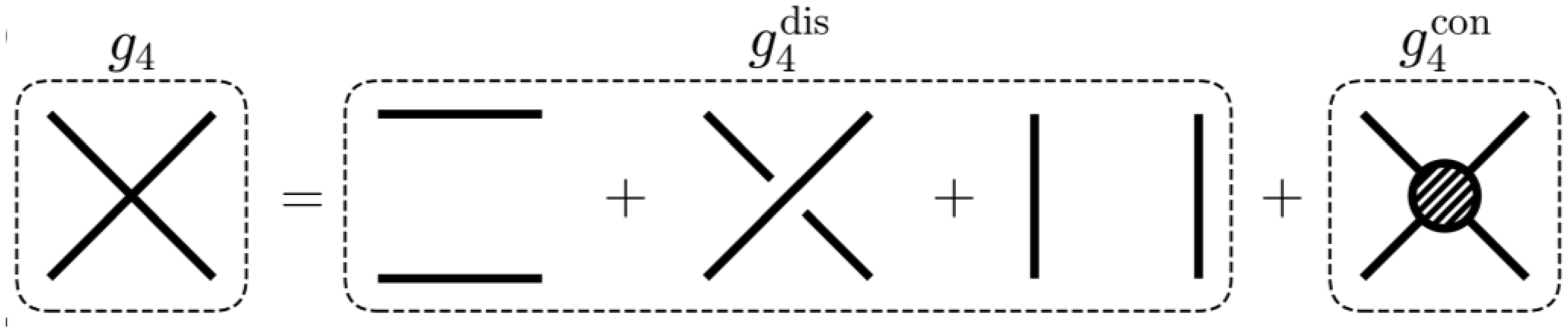

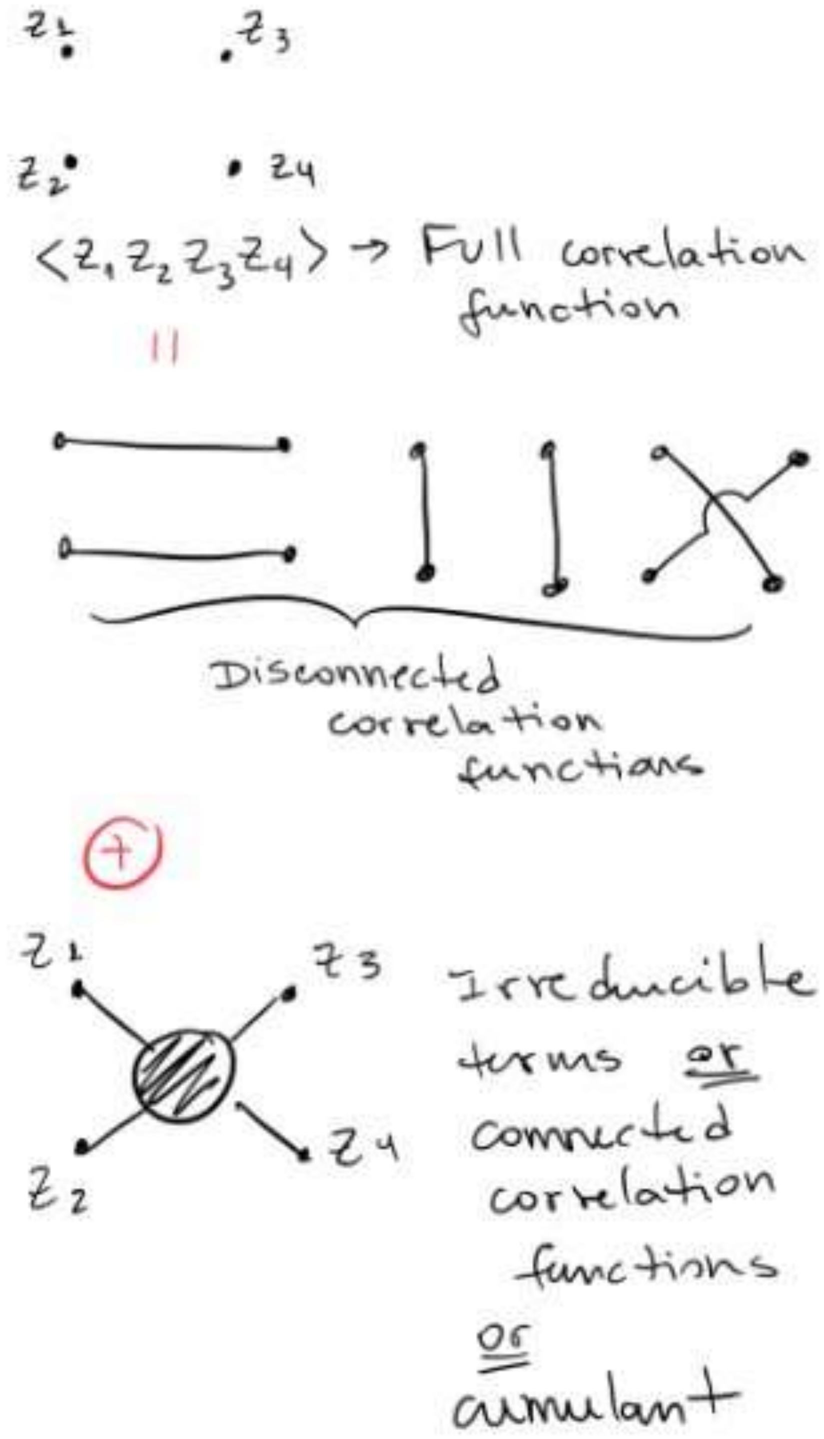

Correlation Functions Analysis

$$\mathbf{STFT}\{x(t)\}(\tau,\omega) \equiv X(\tau,\omega) = \int_{-\infty}^{\infty} x(t)w(t-\tau)e^{-i\omega t}\,dt$$

Short Fourier Transform

- x(t) is a time-dependent signal and w(t) is a window function (Hann.).
- At fixed frequency, the absolute value of the complex amplitude X gives the slow-time envelope of the signal around that frequency, which turns these methods ideal for looking at unstable behaviour at time scales much larger than an oscillation period.
- There are three parameters on the STFT: the window length, the FFT length and the hop time. The window length determines the convolution width of the FFT and the longer the window is, the smoother, but more time-averaged, the slow-time envelopes.
- The FFT length sets the frequency resolution for the spectrogram. The hop time determines the discretisation level of the slow-time, it can as short as the discretisation spacing of the original time array t. Hence, the hop time sets the time resolution of the spectrogram.

Frequency Correlation Functions

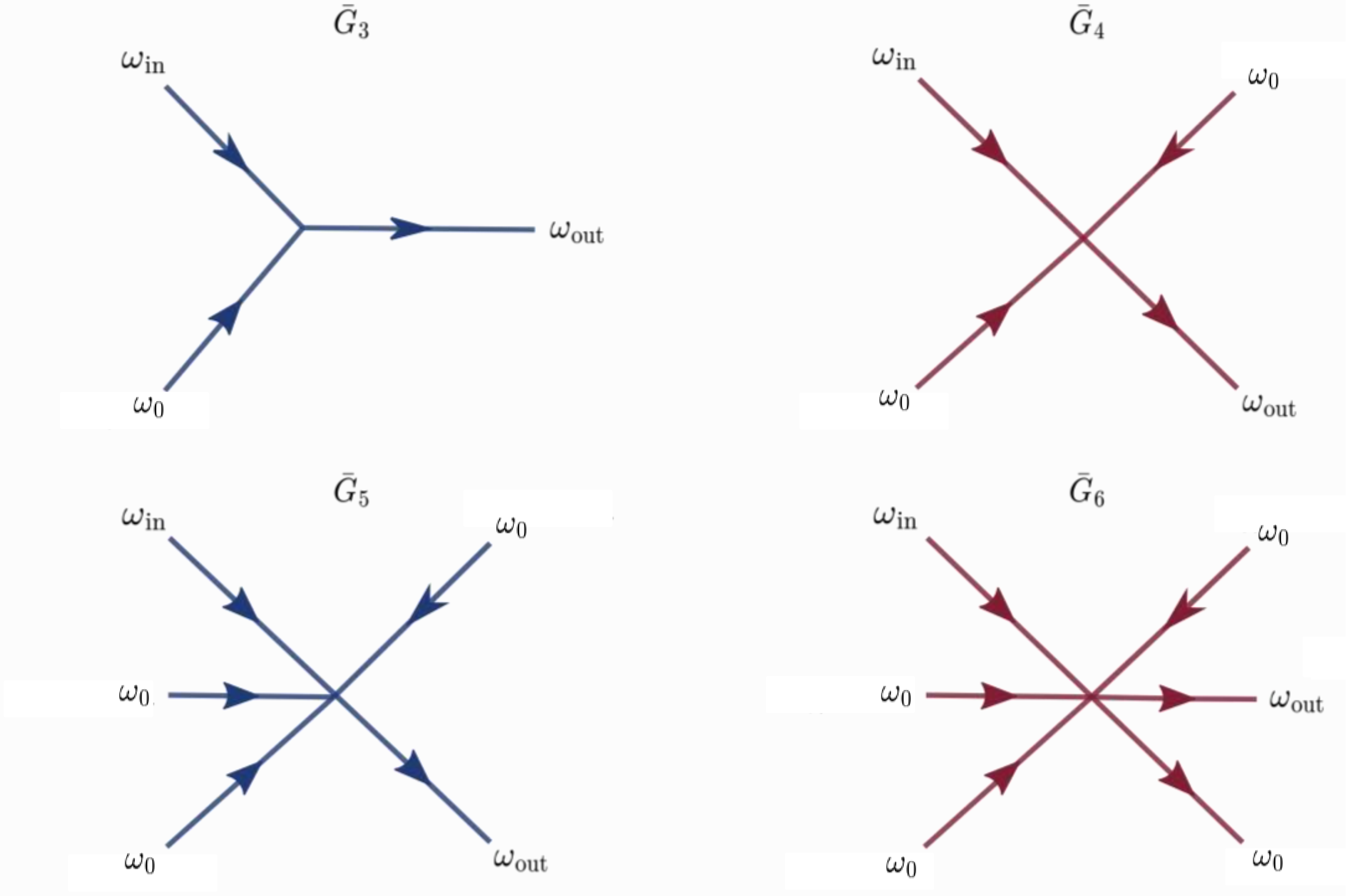

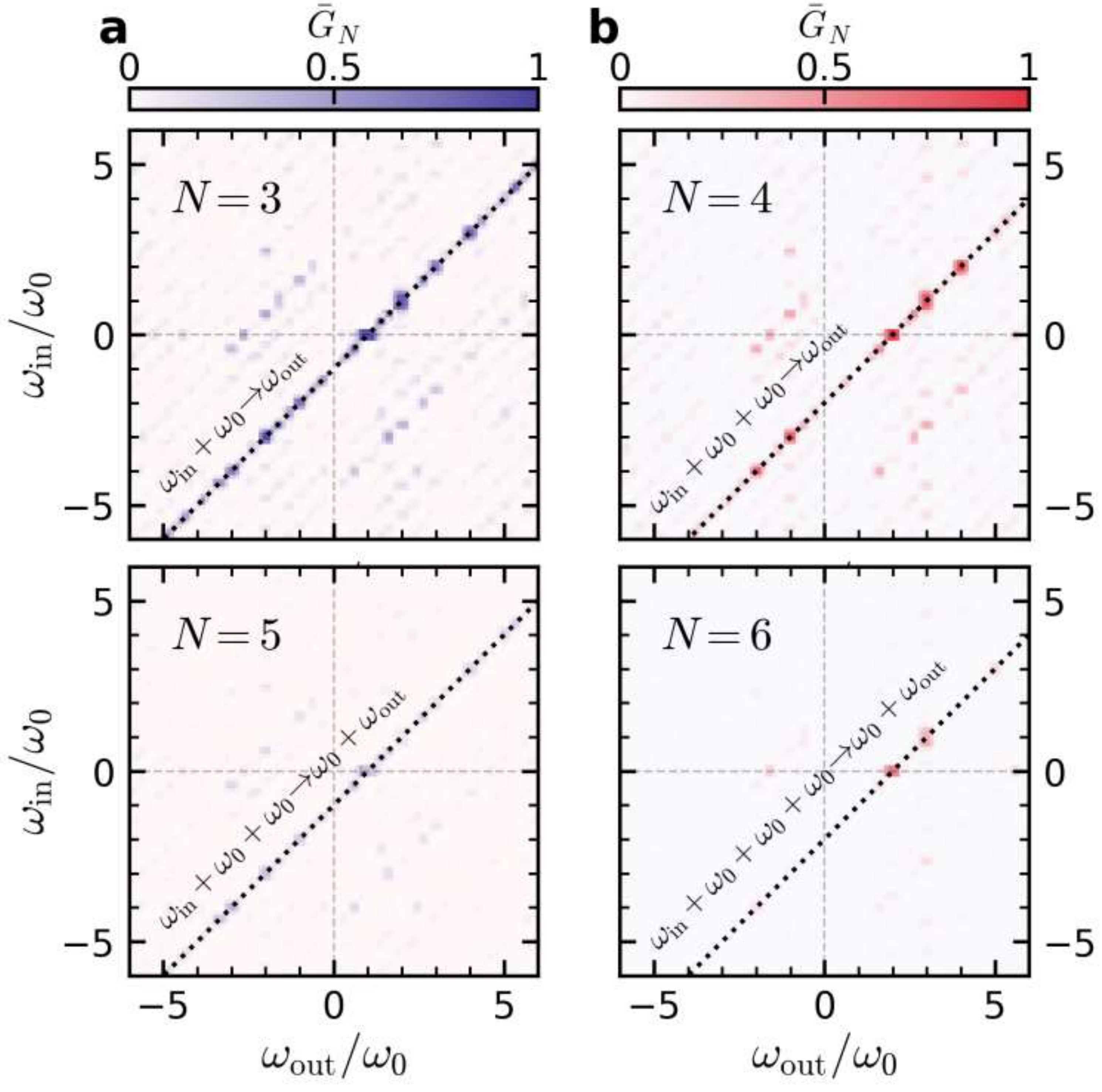

Reduced dynamics

- Energy is injected into one **primary mode** $\xi_1 \sim A(\tau)e^{i\omega t}$ which grows on a slower timescale, τ, than it oscillates, t

- The slow-time amplitude of the primary grows exponentially
$$A(\tau) \propto e^{\lambda t}$$
until it is arrested at $A(\tau_{late}) = A_s$ by nonlinear self-interaction

- Many other modes are excited by the primary, but have considerably smaller amplitude so do not influence the dynamics of ξ_1

- Substituting the form of $\xi_1 = Ae^{i\omega t} + A^* e^{-i\omega t}$ into $L^{(1)}$, then averaging over an oscillation cycle yields a Lagrangian for the slow-time amplitude $A(\tau)$

- To determine the height at which the interface saturates, one discards all modes other than the primary to obtain a **one mode reduced Lagrangian** $L^{(1)}$

- By considering the dynamics of the primary mode alone, one may determine aspects of the entire system, such as the timescale between an initial state $\xi_1 \sim A_0$ and an established cascade:
$$\Delta t = \lambda \log\left(\frac{A_s}{A_0}\right)$$

- Fixed points are found from the resulting equation of motion – this informs the height at which the primary mode saturates

Dynamics and decomposition

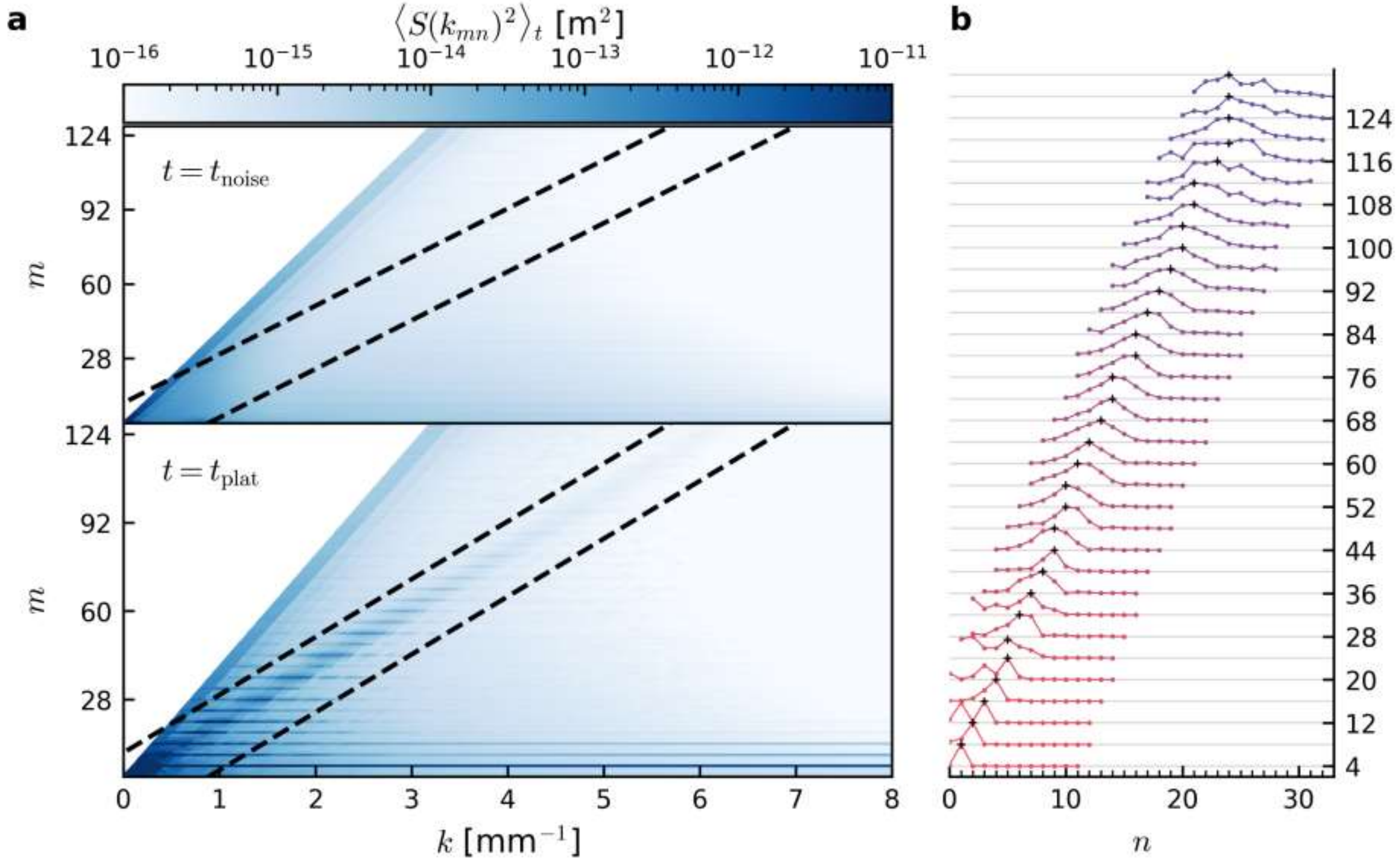

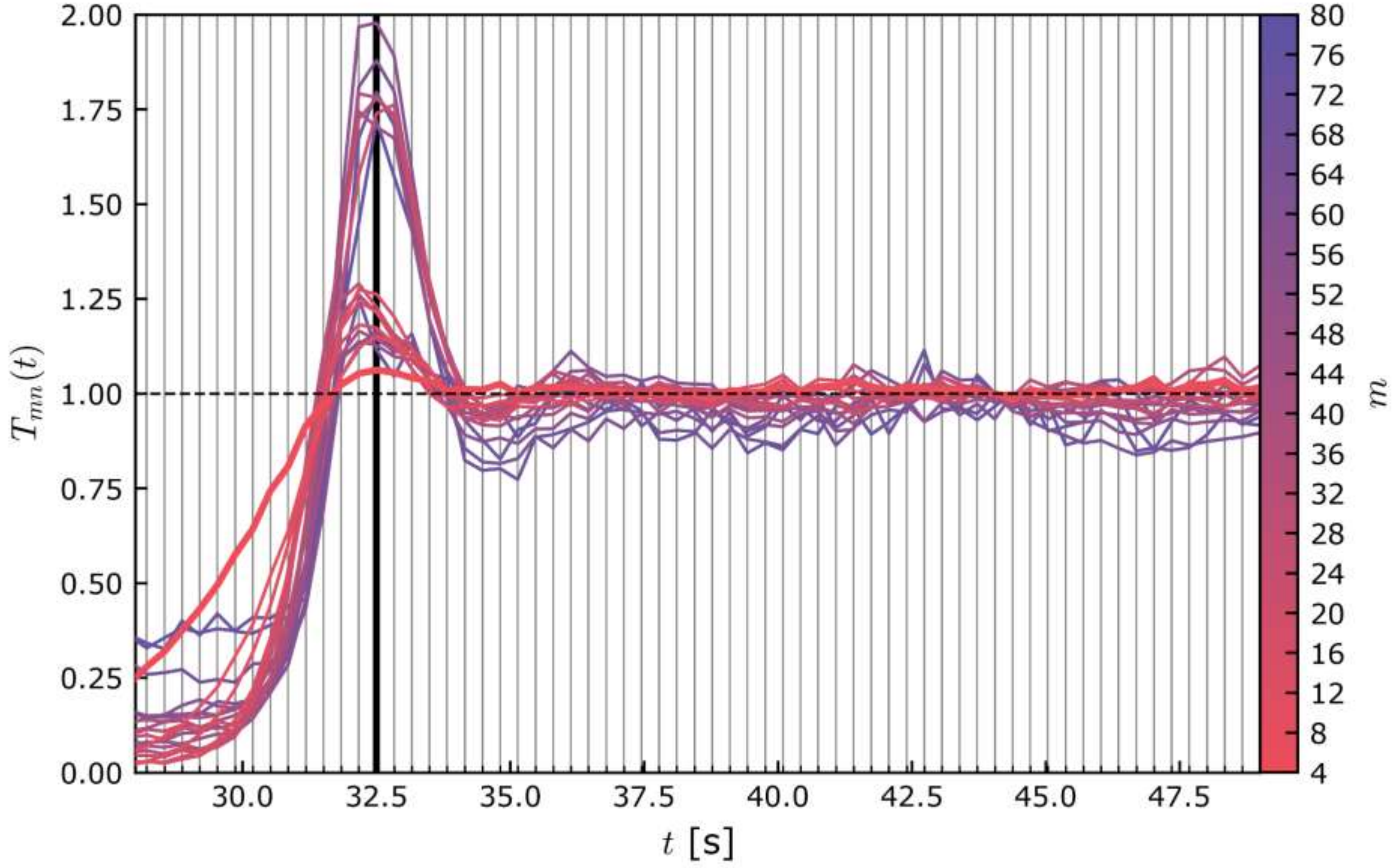

Open Questions

1. How should **correlation functions** for complex fields be calculated? What are the limits of the interpretation for these quantities?
2. Study of **turbulence**: is it possible to obtain a study of the scaling coefficient changing parameters of the system (towards a study of turbulence in finite-size and strong drive)? How can we introduce randomness?
3. To which systems can the **one-mode reduced dynamics** can be applied?
4. **How does things change when more than one mode is excited parametrically?**
5. **Is it possible to change the shape of the drive?**
6. **How to do it in (3+1)? What does and doesn't change in the passage from (2+1) and (3+1)?**
7. **How do we make it more in line with the cosmological scenario? We keep driving, free slip BC such that the profile of the mode resambles that of the velocity potential (neumann) makes clearer the match between theory and experiment, lower viscosity to observe decay, brpadband**